The Scattering of Phonons by Dislocations

A. C. Anderson

Department of Physics and Materials Research Laboratory

University of Illinois at Urbana-Champaign

Urbana, Illinois 61801

United States of America

Suggested abbreviated title: Phonon Scattering

63.20.Mt

DISCLAIMER

Contents

List of Symbols

A	cross-sectional area of sample
$^{\circ}C$	celsius temperature units
ΔC	change in specific heat
$C(\omega)$	specific heat of phonons of frequency ω
G	length of sample
$\hbar$	Planck constant divided by 2π
K	Kelvin temperature units
k	Boltzmann constant
L	average segment length of dislocation between pinning points
ℓ_n	net phonon mean free path
ℓ_B	phonon mean free path ascribed to scattering from sample surfaces
ℓ	phonon mean free path
N	dislocation density
$\dot{Q}$	heat flux
T	temperature
T_c	superconducting transition temperature
ΔT	temperature difference
T_{min}	temperature at which ℓ exhibits a minimum due to a resonant scattering process
v	acoustic phonon velocity
θ,ϕ	angles of phonon incidence
κ_{ph}	phonon thermal conductivity
κ_{el}	electronic thermal conductivity
κ_B	phonon thermal conductivity of undeformed sample
κ_{tot}	total thermal conductivity
ρ	electrical resistivity
τ	mean lifetime between phonon scattering events
ω	phonon frequency divided by 2π
$\Delta\omega$	spectral width

1. Introduction

By 1950, an explicit effort had been launched to use lattice thermal conductivity measurements in the investigation of defect structures in solids [1]. This technique has been highly successful, especially when combined with the measurements of other properties such as optical absorption [2]. One exception has been the study of dislocations. Although dislocations have a profound effect on the phonon thermal conductivity, the mechanisms of the phonon-dislocation interaction are poorly understood. The most basic questions are still debated in the literature. It therefore is pointless to attempt a quantitative comparison between an extensive accumulation of experimental data on the one hand, and the numerous theoretical models on the other. Instead, this chapter will attempt to glean a few qualitative conclusions from the existing experimental data. These results will then be compared with two general models which incorporate, in a qualitative manner, most of the proposed theories of the phonon-dislocation interaction.

It may well be asked, if the thermal-conductivity technique is so nondefinitive, why is it used? The answer is simple. Until very recently, measurement of thermal conductivity was the only means available to probe the interaction between phonons and defects at phonon frequencies above the standard ultrasonic range of $\approx 10^9$ Hz. The following introductory paragraphs provide a brief review of the thermal-conductivity technique and the problems which are encountered in practice. There is also a brief presentation of the theoretical models and the complications that may occur in more realistic situations. These introductory paragraphs are included

so that the reader may better understand why so little information has been derived from so much effort.

1.1. The thermal-conductivity technique

In a crystalline material free of defects, the phonons which make the largest contribution to the low-temperature phonon thermal conductivity κ_{ph} have an angular frequency ω of $\omega \approx 4kT/\hbar$, where T is the absolute temperature, k is the Boltzmann constant and $\hbar$ is the Planck constant divided by 2π. This is the phonon analogue of Wien's displacement law in black-body radiation. In essence, a measurement of κ_{ph} versus T is equivalent to the use of a broad-band phonon spectrometer of spectral width $\Delta\omega \approx 4kT/\hbar$ in which the central frequency ω is varied by adjusting T. In this sense, the thermal conductivity of a crystal containing a defect may be used to infer the magnitude and frequency dependence of the phonon-defect interaction.

1.1.1. Analysis of thermal conductivity data

The "dominant-phonon" concept outlined above, wherein $\omega \approx 4kT/\hbar$, is very useful and will be employed in this paper. But the concept is, in general, too simplistic and has led to erroneous conclusions in the past. It should be recognized that the low-temperature phonon thermal conductivity is a rather complicated property given by

$$\kappa_{ph} = \frac{1}{3} \sum_i \int C_i(\omega) \quad v_i^2(\omega) \; \tau_i(\omega) \; d\omega \qquad (1)$$

where the sum is over the longitudinal and two transverse acoustic phonon modes, $C_i(\omega)\, d\omega$ is the contribution to the specific heat by phonons of mode i in the frequency range between ω and $\omega + d\omega$, and $v_i(\omega)$ is the velocity of

mode i at frequency ω. The term $\tau_i(\omega)$ is the mean time duration between scattering events for phonons of frequency ω and mode i. If a defect is present, $\tau_i(\omega)$ contains the desired information concerning the interaction between thermal phonons and that defect.

Obviously it is not possible, using Eq. 1, to deduce $\tau_i(\omega)$ from the measured thermal conductivity unless a great deal of ancillary information is available concerning $C_i(\omega)$ and $v_i(\omega)$. To reduce the amount of information required, the Debye approximation is generally adopted. In this approximation it is assumed that $v_i(\omega)$ is a constant, $v_i(\omega) = v_i$. As a result $C_i(\omega) = (k\omega^2/2\pi^2 v_i^3)x^2\, e^x(e^x-1)^{-2}$ with $x = \hbar\omega/kT$. This approximation is reasonable for $T \lesssim 10$ K and, in an isotropic solid, requires only a measurement of the three v_i at ultrasonic frequencies. In general, the integration over ω in Eq. 1 must be carried out explicitly. However, in the event that $\tau_1(\omega)$ is a weak function of ω, $\kappa_{ph} \approx (1.36 \times 10^{12}T^3) \sum_i \tau_i(\omega)v_1^{-1}$, in units of W/mK*, with $\omega = 4kT/\hbar$. This represents one form of the dominant-phonon approximation.

For a given defect, the phonon-defect interaction may not be the same for the three phonon modes. Hence $\tau_i(\omega)$ may depend explicitly on i as well as ω. In this situation it is possible that the most <u>weakly</u> scattered phonon mode will dominate the thermal conductivity, contrary to what is occasionally stated in the literature. It may not be possible to obtain any quantitative information concerning the stronger phonon-defect interaction. This problem will be encountered in Sec. 2.1.1.

If all three phonon modes were to undergo the same interaction with the defect, then $\tau_i(\omega) = \tau(\omega)$ could be deduced from the measured κ_{ph}

*All units in this chapter are MKS.

provided only one process of phonon scattering were dominant. Often, however, more than one scattering process may be present. It is then assumed that $\tau_i(\omega)^{-1} = \sum_j \tau_{ij}^{-1}(\omega)$, although this approximation does occasionally fail [3]. To find a specific τ_{ij} it is essential to have detailed information about all other τ_{ij}. Generally this is not possible. The literature, unfortunately, contains many analyses in which several terms in $\sum_j \tau_{ij}^{-1}$ are treated as adjustable parameters. Such an analysis is a numerical exercise devoid of physical information.

Thus far in this discussion the crystalline sample has been treated as isotropic. The anisotropy of the crystal does produce an important anistropy in κ_{ph} [4]. Furthermore, the phonon-defect interaction may itself depend on the direction of propagation of the incident phonon [5]. Hence $\tau_i(\omega)$ becomes $\tau_i(\omega, \theta, \phi)$.

The foregoing paragraphs should convince the reader that it is difficult at best to obtain quantitative information about the phonon-dislocation interaction from thermal-conductivity measurements. In view of the difficulties involved in the analysis of data, it should not be surprising that disparate conclusions have been reached by different authors. In addition, there is the underlying problem as to the reliability of the data on which the conclusions are based. This question is discussed in the following section.

1.1.2. The measurement of thermal conductivity

Thermal conductivity is measured as a function of temperature. Other variables occasionally used, such as electric or magnetic fields, are not of interest here. A schematic experimental arrangement is shown in Fig. 1

where R represents the refrigerator and S the sample. In one scheme B_1 and B_2 are thermometers, separated by a distance G, which measure a temperature difference ΔT created by a heat flow $\dot{Q}$ introduced by the electrical heater C. Then $\kappa_{tot} = \dot{Q}G/A\Delta T$, where κ_{tot} is the total thermal conductivity for the region between B_1 and B_2 and A is the cross-sectional area of the sample. Alternatively, B_1 and B_2 may be heaters and C a thermometer which measures the temperature increase ΔT when power $\dot{Q}$ is switched from B_2 to B_1.

Errors in the measurement of $\dot{Q}$, G and A are generally small and of little consequence. The most important error, in practice, is in ΔT. Errors in ΔT have led to the publication of papers purporting to show anomalous variations in the temperature dependence of the thermal conductivities of various materials, variations which do not, in fact, exist [6,7,8]. The source of such an error is not always obvious. Some experimentalists use carbon resistance thermometers which are known to drift with time [9]. Others rely on the calibration of commercial thermometers. Such thermometers have been found to be in error by as much as 50% [10]. Any low temperature measurement (at least prior to 1979), which relies on the calibration of a commerical thermometer, must be suspect.

There is also a more subtle thermometry problem which is especially important in measurements of metals. The thermal conductivity of a metal may be written $\kappa_{tot} = \kappa_{ph} + \kappa_{el}$, where κ_{el} is the contribution from conduction electrons which must be subtracted from κ_{tot} to obtain the desired κ_{ph}. A measurement of the low-temperature electrical resistivity ρ provides a value for κ_{el} by use of the Weidemann-Franz relation, $\kappa_{el} = 2.45 \times 10^{-8}\ T\ \rho^{-1}$.

But it must be noted that the subtraction $\kappa_{tot} - \kappa_{el}$ involves two different temperature scales. That in the Wiedemann-Franz relation is the thermodynamic, absolute temperature whereas κ_{tot} is measured using a laboratory temperature scale. This difference is significant since κ_{el} and κ_{tot} have so nearly the same magnitude that small errors in κ_{tot} are amplified by the mathematical subtraction. Until 1978, the only low-temperature scale universally available was based on the vapor pressure of liquid helium. Even if the experimentalist managed to reproduce this vapor-pressure scale accurately, the vapor-pressure scale itself was in error by an amount ranging from 0.2% at 5 K to possibly $\simeq$ 1% when extrapolation to $T \lesssim 0.1$ K. The situation was improved in 1979 with the availability of precision superconducting thermometric fixed-points [11,12] based on a temperature scale of greater accuracy [13].

In summary, even if experimental errors have been successfully avoided, a measurement of κ_{ph} versus T can tell us little concerning a phonon-defect interaction in a crystal unless we also know the kinds and densities of defects present and the phonon modes which interact with those defects. A definitive analysis and comparison with theory will therefore require additional measurements other than thermal conductivity.

1.2. Theoretical models of the phonon-dislocation interaction

In the previous sections the approach has been to deduce $\tau_i(\omega)$ from the measured κ_{ph}. The $\tau_i(\omega)$ might then be compared with theoretical models. However, because of the complexity of phonon thermal transport, it is mathematically more simple to calculate a κ_{ph} by substituting the theoretical $\tau_i(\omega)$ in Eq. 1 and then to compare the calculated κ_{ph} with

the experimental result. This latter approach will be adopted in this section.

It is convenient to think of two general types of phonon-dislocation interactions, namely "static" and "dynamic". In the static interaction the position of the dislocation does not change, relative to the crystalline lattice, as a phonon passes. In the dynamic interaction the dislocation, in some sense, moves relative to the lattice because of the influence of the time-dependent stress field of the passing phonon. Within this definition, any dislocation which undergoes a dynamic interaction with a phonon will possess an associated localized-mode or vibration. This localized mode is absent for dislocations which undergo only a static interaction. In the following paragraphs, several explicit models will be mentioned by way of introduction. The list of models is not exhaustive.

1.2.1. The static interaction

Kogure and Hiki [5] provide recent calculations of the static interaction and review the work of others, including the widely quoted work of Klemens [14]. The origin of this phonon scattering mechanism is the nonlinear elastic response of the strained region surrounding a sessile dislocation. The calculation predicts a τ proportional to ω^{-1} or, using Eq. 1, a κ_{ph} proportional to T^2 if this is the only scattering process present in the sample. The theoretical magnitude of the static interaction is somewhat uncertain as will be discussed in Sec. 2.2.

The static interaction is highly anisotropic relative to the direction of phonon incidence and depends on the phonon mode as well as the type of dislocation, i.e. edge or screw [5]. The interaction may also be modified by the presence of impurity atoms (Cottrell atmosphere) [15]. If the

dominant-phonon wavelength becomes camparable to or larger than the distance between dislocations, the scattering magnitude could be either reduced [16,17] or increased [18], depending on the arrangement of the dislocations. Hence, as the temperature is lowered, the temperature dependence of κ_{ph} may deviate from T^2. In like manner, special arrays of dislocations such as grain boundaries might cause a temperature dependence other than T^2. Finally, the phonon-scattering behavior could be modified for an extended or dissociated dislocation [19].

1.2.2. The dynamic interaction

The simplest approach is to view the dislocation as a stretched elastic string which can support the propagation of waves. A passing acoustic phonon of angular frequency ω may then induce on the string a traveling wave of the same frequency. In this manner the dislocation absorbs the energy of the phonon and then reradiates this energy, or phonon, in a different direction, which constitutes a phonon-scattering process. The dislocation does remain in thermal equilibrium at the low temperature of the measurements ($\lesssim$ 10 K). Hence the amplitude of vibration of the dislocation is much smaller than a lattice constant [20], i.e. $\ll 3$ Å ($\ll 3 \times 10^{-10}$ m). The amplitude of thermal vibration is also much smaller than the amplitude attained in ultrasonic investigations of dislocations.

Ninomiya [21] has treated the case of the infinite, isolated dislocation, while Granato [22] has considered the enhanced scattering which occurs when the dislocation is pinned at discrete points so as to leave segments of an average length L free to flutter. A mechanical

resonance then occurs at a frequency of $\omega \simeq v/L$ and the phonon lifetime τ would exhibit a minimum near this same frequency. In the dominant-phonon approximation, κ_{ph}/T^3 would have a minimum near $T \simeq \hbar\omega/4k \simeq \hbar v/4kL$ as a consequence of the resonance.

The frequency dependence described above could be further complicated if the local density of dislocations were sufficiently large to permit correlations between different scattering events as, for example, in a dislocation dipole [23,24] or in a grain boundary [25]. Alternatively if individual, isolated dislocations were dissociated, there could occur internal degrees of freedom and their related vibrational motions [26,27]. In addition, the dislocation motion may be influenced by the undulatory Peierls-Nabarro lattice potential experienced by the dislocation which might, in turn, require the consideration of kink motion [28].

In the following sections, the scattering magnitude calculated by Granato [22] will be adopted as a theoretical value typical of all resonant dynamic processes. If the minimum in $\kappa_{ph}T^{-3}$ occurs at T_{min} because of the resonance, then τ at T_{min} is given, very roughly, by $\tau \simeq 10^{12}\ T_{min}/N\ v^2$, where N is the dislocation density. This approximate relation is applicable to the temperature range of $T_{min} \simeq 0.1 - 1$ K.

1.2.3. A comparison of the static and dynamic interactions

In general, the dynamic process causes much stronger phonon scattering than the static mechanism, at least for phonons having frequencies near the resonant frequency of the dislocation. The temperature dependence of κ/T^3 should be T^{-1} for the static mechanism, whereas κ/T^3 should display a minimum for the dynamic mechanism. These are signatures

which, if present in the measured thermal conductivity, suggest the type of interaction which may be present. However, as noted previously, other temperature dependencies could be associated with the phonon-dislocation interaction.

2. Experimental results and comparison with theoretical models.

The most thoroughly studied crystal system, the ionic alkali halides, will be discussed first. Next, covalent crystals and superconducting metals will be reviewed. Like the alkali halides, measurements on these materials are not encumbered by a contribution from conduction electrons. Normal metals, the most difficult system to analyze, will then be discussed, followed by a few miscellaneous examples. A comparison of the experimental results with the two generalized theoretical models will be offered with each class of material.

The few conclusions which can be gleaned from this presentation will be found in Sec. 3. In light of the past history of this subject, it is unlikely that these conclusions will be met with universal acceptance. Therefore, explicit indications are made as to where additional work could be constructive in providing more definitive information.

The numerical data provided in the following pages is often qualitative, but is generally accurate to within a factor of ≈ 2. Also, some details of the experimental thermal conductivity results have been ignored. These details may reveal the influence of more complex and subtle phonon scattering mechanisms. Nevertheless, we seek here to determine only if the dominant scattering mechanism is static or dynamic in each example.

2.1 Ionic crystals

As indicated above, the most thoroughly studied system has been the alkali halide crystals. Of this class, work on LiF has been the most fruitful.

2.1.1. LiF

In undeformed, annealed crystals of LiF at temperatures below ≈ 5 K, the phonons scatter only from the surfaces of the samples [28,29]. At higher temperatuees there may occur point-defect scattering from isotopic Li impurities [30]. When a LiF crystal is deformed by shearing in a manner indicated by the inset in Fig. 2, the thermal conductivity is reduced to a fraction of its original magnitude because of the introduction of dislocations into the sample. This reduction is shown by curve A in Fig. 2, where the thermal conductivity of the deformed sample, κ_{ph}, has been divided by the thermal conductivity of the undeformed sample, κ_B. This normalization proceedure has two advantages. First, it removes most of the temperature dependence. Thus the vertical scale may be greatly expanded. Second, it emphasizes the changes caused by deformation or other treatment of the sample.

The deformed LiF samples were next subjected at room temperature to successive exposures of γ-irradiation. The purpose of the γ-irradiation was to introduce point defects which, from ultrasonic measurements [31,32], are known to pin the dislocations and hinder macroscopic motion. The curves B and C of Fig. 2 show that γ-irradiation restores κ_{ph} to the magnitude which existed prior to irradiation.

Finally, the densities of isolated dislocations were deduced from etch-pit counts on both the (001) exterior surfaces of the samples and from interior (100) surfaces exposed by cleaving through the deformed region of each crystal. Etch-pit determinations of dislocation densities have been found to give good agreement with other techniques [33]. The

density was $\approx 4 \times 10^{11}$ m^{-2}, and the dislocations were primarily edge type aligned perpendicular to the (001) face.

The following experimental facts have been obtained from a series of measurements on LiF crystals deformed by "shearing".

(a) The introduction of dislocations reduced κ_{ph} to roughly 50% of its magnitude prior to deformation.

(b) This 50% reduction was <u>independent</u> of the density of dislocations.

(c) The magnitude of κ_{ph} (at a given temperature) was proportional to the width of the sample <u>in the deformed state</u> as well as in the undeformed state.

These three results can be explained in only one way. A fraction of the thermal phonons is scattered so strongly by the dislocations that this fraction makes essentially no contribution to κ_{ph}, while another fraction is so weakly scattered by the dislocations that, for a dislocation density of $\approx 10^{11}$ m^{-2}, this fraction continues to be scattered only by the surfaces of the sample as in the case of the undeformed specimen. Hence this latter, weakly scattered fraction completely dominates κ_{ph} in the freshly deformed samples (for $T \gtrsim 0.04$ K).

The slow-transverse phonons in undeformed LiF contribute roughly 45% of the thermal conductivity, while the fast-transverse phonons contribute $\approx$ 40% and the longitudinal $\approx$ 15%. These values are obtained from the three respective terms in Eq. 1. The reduction to $\approx$ 50% of the magnitude of κ_{ph} observed prior to deformation, and the fact that the Peach-Koehler relation [34] indicates that the slow-transverse

phonons should interact most strongly with the edge dislocations, suggest that the slow-transverse phonons may be the strongly scattered fraction. The thin layer of dislocations in these LiF samples would thus act like a filter responsive to the polarization vector of individual phonons. This behavior is analogous to the performance of a Polaroid filter in the field of optics.

A direct test was made to determine if the slow-transverse phonons were being scattered most strongly [28]. On one end of a LiF sample a thin metallic electrical heater was vapor deposited. A fast-response thermometer or bolometer was applied to the opposite side. One short pulse of power to the heater created three phonon pulses, one for each of the three acoustic phonon modes. The pulses propagated ballistically through the sample at their respective velocities. The thermometer then recorded three time-resolved spikes as shown in Fig. 3. When the sample was deformed by shearing, as in the inset of Fig. 2, the spike corresponding to the slow-transverse mode decreased in magnitude relative to the other two modes as shown by the lower trace in Fig. 3. Exposure to γ-irradiation restored the slow-transverse spike. Hence there is direct evidence that, in LiF deformed by shear, the slow-transverse thermal phonons are scattered by the presence of edge dislocations with greater strength than the other two modes.

Crystals of LiF were also deformed by bending about an [001] axis [29,35]. Etch-pit counts again indicated a dislocation density of roughly 10^{11} m^{-2}, but with possibly 1/4 of these being screw dislocations. The results following deformation and following γ-irradiation are shown by curves D and E of Fig. 2, respectively. The depressed thermal conductivity of a freshly bent sample, curve D of Fig. 2, has been shown to extend to 25 K [35].

The three results (a), (b), and (c) listed above for sheared crystals were also observed for the bent crystals, but with one difference. The reduction in κ_{ph} was to about 40% of the magnitude of the undeformed crystal as may be seen in Fig. 2. A simple explanation is that both the slow-transverse and the longitudinal phonon modes are strongly scattered by the different array of dislocations in bent samples, leaving only fast-transverse phonons to carry the heat. This suggestion, however, has not been verified by using ballistic-phonon measurements.

An additional fact may be obtained from the measurements on sheared and bent LiF crystals.

(d) The temperature region above which the slow-transverse phonons are strongly scattered by dislocations is increased with increased exposure to γ-irradiation.

For curve C of Fig. 2 the dislocations are still present, but the slow-transverse phonons are now scattered by the sample surfaces just as in the undeformed sample. Clearly the phonon-dislocation interaction has been significantly modified by the pinning effect of the γ-induced point defects. The only explanation advanced thus far is that the interaction of phonons with fresh dislocations is dynamic in character, and that successive γ-irradiations push the dislocation resonances to higher frequencies. The increase in resonant frequency is perhaps caused by a reduction in the lengths of dislocations, between pinning points, which are free to flutter.

Although the data are much less conclusive, it does appear that pinning of dislocations by heat treatment, that is, through pinning

caused by the thermal diffusion of impurities to dislocations, produces essentially the same behavior below 1 K as does γ-irradiation [29].

Earlier measurements on LiF obtained at temperatures above 1.5 K showed a reduction in κ_{ph} much larger than 50% following deformation by compression [35,36], see Fig. 4. However, the dislocation densities in these samples were also larger, ranging from $\approx 10^{12}$ to 10^{13} m^{-2}, and the heat flow was along a [100] crystal axis. In Fig. 4, curves A and C represent freshly deformed samples with C having a factor of $\approx$ 3 larger dislocation density than curve A. A mild heat treatment at 300°C reduced the density of dislocations by a factor of about 2, but also changed the temperature dependence as shown by curves B and D of Fig. 4. The ratio of curve B to curve A, or of D to C, in Fig. 4 has a similar temperature dependence as the ratio of curve E to D of Fig. 2. In brief, it would appear that a dynamic phonon scattering process occurs at the freshly produced dislocations in compressed crystals, just as in sheared or bent crystals, and that a mild heat treatment pins these dislocations and moves the resonance to higher frequencies as in the sheared or bent samples.

Still, the conductivity of the compressed samples is reduced by a factor of $\gtrsim$ 20, versus a factor of $\approx$ 2 for sheared or bent crystals, and the magnitude of this depression in compressed crystals appears to be roughly proportional to the density of dislocations, contrary to conclusion (b) above for sheared or bent crystals. One possible explanation is that the fast-transverse phonons in compressed samples continue to dominate κ_{ph} as in the sheared or bent samples, but are limited in mean free path by a relatively weak scattering from the dislocations. Only the larger dislocation densities found in compressed

samples in LiF permit the weaker scattering of the fast-transverse phonons to be detected. The effect of thermal pinning seen in Fig. 4 would then indicate that the interaction of fast-transverse phonons with freshly produced dislocatinns is also dynamic in character as for slow-transverse phonons. An alternative explanation is that all three phonon modes in compressed samples undergo a dynamic scattering of roughly the same magnitude. Measurements of thermal conductivity on compressed samples at temperatures below 1.5 K would be helpful in resolving this question.

In comparing the data with theory, we first focus on the samples which had been γ-irradiated for the greatest length of time. The dislocations are still present, but a depression in κ_{ph} persists only in the temperature range above $\simeq$ 2 K (curves C or E of Fig. 2). If it is assumed that the reduction near 1-2 K is caused by the static scattering mechanism, which produces a T^2 temperature dependence of κ_{ph}, then the experimental lower limit on κ_{ph} due to sessile dislocations is $\kappa_{ph} \geq 2 \times 10^{13} T^2 N^{-1}$ where N is the dislocation density. This is a lower limit on κ_{ph} for the static interaction since the dynamic process may also be present. The static models of Koguri and Hiki [5] or of Klemens [14], which are discussed in greater detail in Sec. 2.2, predict κ_{ph} to be within the range $\simeq$ (3-300) $\times 10^{13} T^2 N^{-1}$, the smaller values being prefered by those authors. Thus any residual scattering which may be present in the fully γ-irradiated samples for $T < 2$ K is consistent with this model of static scattering. On the other hand, a static model which has been developed by Ohashi [37] to predict much stronger phonon scattering, is not applicable to LiF.

We next turn to the freshly deformed samples of Fig. 2 (curves A or D) and Fig. 4 (curves A or C). The static scattering model, such as that of Klemens, does not explain these results. The temperature dependences are wrong, the scattering magnitude is too weak by a factor of $\gtrsim 100$ and the pinning effect is not accounted for. An alternative static-scattering model, one which considers the scattering resulting from a spatial variation in crystal orientation associated with the presence of dislocations, does purport to provide the T^3 temperature dependence observed in Fig. 2 for freshly deformed LiF [38]. However, it has been empirically demonstrated as discussed above that the observed T^3 dependence is caused by scattering of a dominant heat-carrying fraction of the phonons from the sample surfaces. In brief, no static model explains the behavior of κ_{ph} in freshly deformed LiF.

As mentioned in Sec. 1.2.2., the dynamic model gives $\tau \approx 10^{12}\ T_{min}/N\ v^2$ near a dislocation resonance (See also Ref. 39). This approximate scattering strength is sufficient to explain the scattering of phonons observed near the average resonant frequency of the dislocations in LiF, provided the scattering is indeed caused by the N individual dislocations observed in etch-pit counts. The increase in resonant frequency with successive γ-irradiations suggests that a "vibrating-string" model is more appropriate than, for example, the internal resonance of a dissociated dislocation or a vibration controlled by the Peierls-Nabarro lattice potential. However, a quantitative comparison [24,29] using explicitly the vibrating-string model of Granato [21,22] indicates that this dynamic mechanism scatters phonons within a frequency interval which is much to narrow to explain the depression observed in κ_{ph}

over the broad temperature range of 0.05 to > 5 K. It has therefore been suggested [24] that edge-dislocation dipoles, which are assumed to be more numerous than isolated dislocations, may provide the strong dynamic scattering observed in these measurements. In this calculation the resonant frequency of a dipole depends both on the distance between pinning points and on the spacing between the two dislocations. A distribution in both quantities can provide the spectral width required to fit the thermal conductivity data.

One additional observation may be significant. The LiF samples deformed by bending were investigated more thoroughly above 2 K than were the sheared samples [29]. For the bent samples it appeared that the strong phonon scattering could not be suppressed at temperatures above $\approx$ 3 K by γ-irradiation (Fig. 2) or by thermal pinning (Fig. 4). In the dominant-phonon approximation this corresponds to frequencies $\geq 3 \times 10^{11}$ Hz, or of phonon wavelengths ≤ 100 Å ($\leq 10^{-8}$ m). It is not known whether this saturation in pinning reflects the maximum density of pinning points which can collect on a dislocation [40], or if it reflects in some manner the microscopic topography of the dislocations. What is more important, the lack of a pinning effect for T > 3 K does not permit us, from experimental data alone, to determine if the phonon-dislocation interaction is static or dynamic in character for phonon frequencies above 3×10^{11} Hz. On the other hand, in a comparison with the available theories, the magnitude of the strong phonon scattering which occurs above 3 K is compatible only with a dynamic mechanism.

In summary, it seems certain that fresh dislocations in LiF scatter phonons by a dynamic process. The interaction is highly mode dependent,

and can be supressed at $T \lesssim 3$ K by pinning the dislocations. This behavior is more readily accounted for by a "vibrating-string" model than by other existing models. Any static scattering that occurs at fully pinned dislocations is consistent with the static model first investigated by Klemens.

2.1.2. Other ionic crystals

The influence of compressional deformation on the thermal conductivity has been measured for NaCl, KCl, and NaF crystals at temperatures above 1.5 K [35,41]. The results are similar to the behavior of LiF samples deformed by compression. That is, the scattering magnitude is large relative to the magnitude expected from the static mechanism. On the other hand, measurements below 2 K on NaCl samples deformed by bending and then heat treated gave results compatible with the static model [25]. However, the heat treatment of these NaCl samples at 250°C may have pinned the dislocations through the diffusion of impurities as in LiF. It is therefore suspected that a dynamic mechanism is present in these crystals for freshly produced dislocations, although it would be useful to have a more convincing demonstration of this conclusion as in the case of LiF.

2.2. Covalent crystals

In no system other than LiF is there sufficient experimental information from which to deduce the scattering of the individual phonon modes in a deformed sample. We shall therefore adopt the common but unsatisfactory approximation that all phonon modes are scattered with roughly the same intensity by dislocations, independent of whether the interaction is static or dynamic. Since an approximation is required, it is also convenient to make one additional but less serious approximation, namely to derive and

plot the average intrinsic phonon mean free path ℓ. Plotting an empirical ℓ rather than κ_{ph} permits a comparison of phonon scattering to be made between samples of different dimensions. The intrinsic phonon mean free path ℓ is extracted from the equation (see Sec. 1.1.1) $\kappa_{ph} = 1.36 \times 10^{12} T^3 \ell_n \sum_i v_i^{-2}$ with $\ell_n^{-1} = \ell^{-1} + \ell_B^{-1}$, where ℓ_B is the mean free path that would exist if only boundary scattering were present [42], and ℓ_n is the net mean free path due to all scattering processes.

Measurements obtained at temperatures above 1.5 K from germanium crystals subjected to tensile deformation [43] are represented by the solid curve in Fig. 5. The relation $\kappa_{ph} = 3.2 \times 10^3 \ell_n T^3$ was used to obtain ℓ. Independent measurements at temperatures below 1 K, on a sample deformed by bending, provided a lower limit on ℓ [44]. The dislocation density was estimated to be $\approx 10^{11}$ m^{-2} from the radius of curvature of the bend. When scaled to a density of $\approx 2 \times 10^{13}$ m^{-2} appropriate to Fig. 5, this lower limit on ℓ lies within a factor of 2 of the data at higher temperatures as shown by the dotted line.

From Fig. 5 it is observed that, in germanium for temperatures below $\approx$ 10 K, ℓ is proportional to T^{-1} and hence κ_{ph} is proportional to T^2. A similar result has been reported for silicon [5]. The T^2 temperature dependence of κ_{ph} is that expected from a static phonon-dislocation interaction. Indeed, a low-frequency resonance or dynamic interaction would not be expected in silicon or in germanium because of the large undulating Peierls-Nabarro lattice potential which is present. In brief, the dislocation would be expected to act somewhat like a long rod sliding from side to side in a quadratically-shaped trough of very steep sides. A

naive calculation of the resonant frequency of this motion in germanium gave $\approx 3 \times 10^{11}$ Hz [44]. A single, slight depression in the measured κ_{ph} of germanium near $\approx$ 15 K [43] indicates that the resonant frequency, if it does exist, must lie at a frequency near or above $\approx 10^{12}$ Hz in the dominant-phonon approximation. Thus only a static interaction should be important at temperatures below $\approx$ 15 K.

A comparison of the measured conductivity of $\kappa_{ph} T^{-2} N \approx 3 \times 10^{13}$ with theoretical values of the static interaction is not simple. Klemens corrected [14] his original calculation [45] of the static interaction by reducing the theoretical value of $\kappa_{ph} T^{-2} N$ by a factor of 16. Klemens believes this factor to be reliable [46], but others are not convinced [5]. The corrected value for silicon is $\approx 3 \times 10^{13}$. The calculation of Koguri and Hiki [5] gives $\approx 300 \times 10^{13}$ for silicon, but these authors argue that only the slow-transverse phonon contribution to κ_{ph} of the deformed sample should be considered because this mode has the smallest velocity and hence makes the largest contribution to κ_{ph}. (See the discussion of the Debye approximation in Sec. 1.1.1). The transverse phonon fraction would be $\approx 30 \times 10^{13}$, or possibly a factor of 4 smaller depending on the direction of heat flow relative to the crystalline axis. However, the effect of the smaller acoustic velocity was already included in their original value of 300×10^{13}. Hence the reduction by an effective factor of 10 seems unwarranted. Finally, both Klemens value and that of Koguri and Hiki might be reduced by another factor of $\approx$ 3 for random orientations of dislocations [5,47]. The final theoretical values for silicon (and germanium) then lie between roughly 1×10^{13} and 45×10^{13} for Klemens, and 3×10^{13} and

300×10^{13} for Koguri and Hiki. In each case, the respective authors argue for the smaller values. The value of $\kappa_{ph} T^{-2} N = 1 \times 10^{13}$ corresponds to a phonon mean free path represented by the dashed line in Fig. 5; this value is in order-of-magnitude agreement with the measured mean free path.

In summary, only the static phonon-dislocation interaction is expected to occur in germanium at low temperatures. Hence germanium should be an ideal material for which the "static" theory and experiment may be compared. The experimental results do, in fact, agree with the smallest theoretical values of $\kappa_{ph} T^{-2} N$ calculated for phonon scattering by the strain fields of isolated, sessile dislocations. For this reason the smallest theoretical values of $\kappa_{ph} T^{-2} N$ will be used hereafter in this chapter in the comparisons with experimental data.

2.3. Superconducting metals

In superconducting metals at temperatures well below the superconducting critical temperature, T_c, thermal transport is provided by phonons as in nonmetallic crystals. As T_c is approached, two effects become important. First, the increasing density of conduction electrons scatters phonons. Second, the increasing density of conduction electrons contributes to the thermal conductivity. As a result of these two effects, useful information regarding the phonon-dislocation interaction is generally limited to $T < T_c/4$.

2.3.1. Tantalum

The mean free paths of phonons in tantalum, as limited by dislocation scattering plus conduction-electron scattering, are shown in Fig. 6 [39,48]. The mean free paths have been obtained from the equation $\kappa_{ph} = 7.7 \times 10^3 T^3 \ell_n$.

The temperature dependence of curves A, B and C in Fig. 6 is indicative of a dynamic dislocation scattering mechanism, not a static mechanism. A bent sample, from which curve C was obtained, was sectioned in the deformed region to provide an etch-pit count of $\approx 3 \times 10^{11}$ m^{-2}. At a resonance, the approximate relation $\ell = v\,\tau \approx 10^{12}\, T_{min}/N\, v$ is obtained from the dynamic model (Sec. 1.2.2). This relation therefore predicts $\ell \approx 6 \times 10^{-4}$ m at $T_{min} = 0.33$ K for curve C of Fig. 6. The measured value is 4×10^{-4} m, which agrees well with the value expected for a resonant interaction but is a factor of $\gtrsim 10^2$ too small to be accounted for by the static mechanism. In brief, there is good evidence that the phonon-dislocation interaction in superconducting tantalum is dynamic in nature.

The resonant frequency of the dislocations in tantalum appears to increase slightly with increasing strain, as indicated by curves A, B, and C of Fig. 6. If the pinning were caused by the intersection of dislocations, the mean distance ℓ between pinning points might be expected to vary as $N^{-1/2}$. Hence the frequency would vary as $\sqrt{N}$. Indeed, if the dislocation density for curve A is $\approx 1 \times 10^{11}$ m^{-2} (similar to curve E, see below) whereas that of curve C is $\approx 3 \times 10^{11}$ m^{-2}, the resonance should shift from 0.17 K for curve A to 0.3 K for curve C. The minimum in curve C falls at 0.33 K. The agreement is reasonable, but the proposed explanation is highly speculative.

The temperature dependence of curve D of Fig. 6, which is for a cold-rolled sample, corresponds to κ_{ph} proportional to T^2. This temperature dependence is indicative of a static scattering mechanism, although the data are available for only a small temperature range. The density of

dislocations required to produce curve D would be $\simeq 10^{14}$ m^{-2} if, again, the smallest theoretical value of κ_{ph} T^{-2} N is adopted. A dislocation density of $\geq 10^{14}$ m^{-2} would indeed by reasonable for a cold-rolled sample. Hence the available data suggest that the resonant frequency of dislocations in tantalum increases with increasing dislocation density N and, if N is sufficiently large, only the static mechanism remains for $T \leq 1$ K, i.e. for phonons of frequency $\leq 10^{11}$ Hz. This suggestion is also highly speculative. Additional data below 1 K at large N would be helpful.

It is difficult to prepare and insert an annealed, pure metallic sample into a cryostat without some dislocations being introduced accidentally. If the strong scattering resulting from a dynamic phonon-dislocation interaction is present, the thermal conductivity of a superconductor could be depressed below the value expected from boundary scattering alone. Observations of a depressed thermal conductivity in superconducting tantalum and niobium over a limited temperature range, such as curve E of Fig. 6, had led initially to the suggestion that some new, unknown phonon scattering center must be present [49]. However, when measurements are extended to lower temperatures where the dominant-phonon frequencies lie well below the dislocation resonance, it has been experimentally verified that scattering by the sample surface does reappear, as expected, in tantalum [39] and in niobium [3]. Therefore, the postulation of a new scattering center is not warranted.

2.3.2. Aluminum

The phonon mean free paths in superconducting aluminum samples, measured by two very different techniques, are shown in Fig. 7 [50] where the

relation $\kappa_{ph} = 2.7 \times 10^3 \ell_n T^3$ has been used. The temperature range for aluminum is severely limited by the low T_c of 1.2 K.

The dislocations of curve A in Fig. 7 were introduced by bending the sample at room temperature, while those of curve B were introduced at low temperature by differential thermal contraction. The bent sample was sectioned to obtain an etch-pit count; a dislocation density of $N \approx 10^{10}$ m^{-2} is appropriate to curve A. Although one might argue that the temperature dependence seen in Fig. 7 is close to the T^{-1} expected from the static phonon-dislocation interaction, the measured density of dislocations is too small by a factor of $\approx 10^4$. The dynamic model, on the other hand, is more consistent both with the observed temperature dependence and with the observed magnitude. Using the approximate relation $\ell = \tau v \approx 10^{12} T_{min}/N v$ at the resonance gives $\ell \approx 10^{-2}$ m if $T_{min} \approx 0.2$ K. This is only a factor of 10 larger than the value of $\approx 1 \times 10^{-3}$ m measured near 0.1 K.

2.3.3. Lead

Lead has a conveniently high T_c of 7.2 K. However, a pure lead crystal can deform under its own weight, and it will also anneal at room temperature. Thus it is difficult to control the density of dislocations. Data from three laboratories are shown in Fig. 8 [39,51,52]. The relation $\kappa_{ph} = 3.4 \times 10^4 \ell_n T^3$ was used to obtain ℓ. The dislocations in the samples represented by curves C and B were introduced at low temperatures by bending or by tension, respectively. Those of curve A were introduced at room temperature by bending. Only the sample of curve A was sectioned to obtained an etch-pit count, the result being $\approx 6 \times 10^{11}$ m^{-2}.

Clearly the static model does not apply to lead. Not only is the observed temperature dependence wrong, but the density of dislocations required to explain the magnitude would be > 10^{14} m^{-2} for curve A as compared to a measured density of ≈ 6 x 10^{11} m^{-2}. On the other hand the dynamic mechanism, represented by the dashed line in Fig. 8, agrees rather well with the data. This calculation used explicitly the vibrating-string model of Granato, the measured dislocation density of curve A, and no adjustable parameters [22]. The calculation assumes only that the dislocation resonance lies below 0.05 K, i.e. below 5 x 10^{9} Hz. The difficulties in working with lead, and the quantitative differences in data from the three laboratories, do suggest caution in accepting the conclusion that a dynamic phonon-dislocation interaction is dominant.

2.3.4. Niobium

Phonon mean free paths associated with dislocation and electron scattering in niobium are shown in Fig. 9 [3,53]. The relation κ_{ph} = 6.8 x 10^{3} ℓ_n T^3 was used to obtain ℓ. In some measurements (curves A and B), the dislocations were introduced accidentally by bending the samples despite careful handling. Etch-pit counts were not made on these samples, but an estimate of the dislocation density based on the radius of curvature of the bent crystals [54] gave a lower limit of ≈ 2 x 10^{10} m^{-2}. (The actual density probably lay between 2 x 10^{10} and 2 x 10^{11} m^{-2} [39]). The decrease in κ_{ph} or ℓ was roughly proportional to strain. The temperature dependence of curves A and B is suggestive of a dynamic phonon-dislocation interaction. The relation

$\ell \approx 10^{12}\ T_{min}/N\ v$ (Sec. 1.2.2) gives $\ell \approx 3 \times 10^{-3}$ m if the resonance falls near 0.5 K, which is in agreement with the measured value of $\approx 2 \times 10^{-3}$ m. The static interaction would require a dislocation density of $\approx 10^{13}\ m^{-2}$, which is much larger than the estimated density of $\lesssim 2 \times 10^{11}\ m^{-2}$.

In samples deformed under tension [53]*, such as curve C of Fig. 9, the temperature dependence of κ_{ph} changed from roughly T^3 to roughly T^2 as the deformation increased, at least in the restricted temperature range above 0.3 K. (See also Ref. 51). After the final deformation, a dislocation density of $\approx 10^{14}\ m^{-2}$ was obtained for the sample of curve C from electron-microscope studies following heavy neutron irradiation and thinning of the sample. Both the temperature dependence and magnitude of curve C are consistent with the static mechanism of phonon scattering. Although the accuracy of the commercial thermometry used at the lowest temperatures for these measurements is questionable (See Sec. 1.1.2), the general trend from a T^3 to a T^2 behavior in these data should be reliable. This apparent trend at $T \lesssim 1$ K from a dynamic phonon scattering mechanism to a static mechanism as the density of dislocations increases was also noted for tantalum in Sec. 2.3.1. Possibly the resonant frequency is increased with increasing dislocation density [55] so as to shift the resonance above 2 K, i.e. above 2×10^{11} Hz. Additional data are needed on superconducting niobium at large and intermediate dislocation densities and at temperatures below 0.3 K.

---

*Several misleading comparisons appear in the discussion section of Ref. 53.

2.3.5. Summary

The preponderance of evidence indicates that a dynamic phonon-dislocation interaction is present in some superconducting metals, at least at small dislocation densities. In view of the work on tantalum and niobium, it is clearly important to trace the scattering behavior over a broad temperature range as the density of dislocations is systematically increased. Such measurements would help to determine if the character of the phonon interaction does in fact change with increasing dislocation density.

2.4. Normal metals

In a typical metal, the conduction electrons completely dominate κ_{tot} unless impurities are added to reduce the mean free paths of the electrons. Thus most measurements are made on single-phase alloys, such as 15% (atomic) or less aluminum in copper. Even so, as discussed in Sec. 1.1.2, severe problems remain in attempting to extract the phonon-dislocation interaction. Of the numerous papers on alloys which appear in the literature, only those which make some independent estimation of the dislocation density will be discussed here.

2.4.1. Copper and Aluminum alloys

Several measurements at temperatures above 1 K on copper alloys deformed under tension give $\kappa_{ph} \approx 3 \times 10^{13} T^2 N^{-1}$, as an average, for dislocation densities ranging from 10^{13} to 10^{15} m^{-2} [56-60]. A similar result has been found for aluminum alloys deformed by swaging [61]. The corresponding phonon mean free path for the copper alloys is shown as curve A in Fig. 10, using $\kappa_{ph} = 5.7 \times 10^3 \ell_n T^3$. In Fig. 10, the phonon mean free path ℓ has

been multiplied by the dislocation density N so that the average phonon-dislocation interaction measured in different laboratories may be compared more simply.

The temperature dependence and magnitude of curve A are both in good agreement with the static scattering mechanism. This curve represents samples of large dislocation densities, $N \gtrsim 10^{14}$ m^{-2}. Curve B, on the other hand, was obtained from bent samples [6] having a measured dislocation density of only $\simeq 10^{12}$ m^{-2}. The magnitude of ℓ N for curve B is much smaller than predicted by the static mechanism (essentially curve A of Fig. 10), and the temperature dependence suggests the occurance of a resonance near 1 K. The approximate relation $\ell \simeq 10^{12}\ T_{min}/N\ v$ for the dynamic mechanism near a resonance predicts $\ell\ N \simeq 3 \times 10^{8}$ m^{-1} compared to the measured value of 0.6×10^{8} m^{-1} at T = 1.0 K. Thus there is again a suggestion, as in tantalum and niobium, that a dynamic mechanism occurs for a small dislocation density and that, for a high density, the static mechanism dominates.

The possibility of a transition from a dynamic to a static scattering mechanism with increasing dislocation density encounters a problem with curve C of Fig. 10. This sample [62] contained a large dislocation density ($\simeq 10^{14}$ m^{-2}) and was treated in the same manner as the samples of curve A, in particular that of Ref. 59. Yet the magnitude and temperature dependence are well explained by the dynamic scattering mechanism. (See also Fig. 4 of Ref. 63). This paradox requires further investigation. A collaboration between laboratories in the exchange of samples would help eliminate questions concerning the validity of such, apparently, incompatible data.

It might be expected that a resonant mode of a dislocation in an alloy would be influenced or suppressed by a segregation of solute atoms about the

dislocations, much as occurs for impurities in LiF (Sec. 2.1.1). However, there is at present no definitive evidence that alloys deformed at low temperatures exhibit a more dynamic type of interaction than those deformed at room temperature [60,64]. Atomic diffusion would be prevented for a deformation performed at sufficiently low temperatures.

The static interaction in alloys may also be influenced by the segregation of solute atoms about dislocations [15]. Limited data obtained on copper-aluminum alloys initially deformed under tension at low temperatures [64] suggest that segregation may decrease ℓ or κ_{ph} by a factor of $\simeq$ 4, i.e. the scattering of phonons is stronger after segregation. Unfortunately, the measurements did not establish a temperature dependence of the measured κ_{ph} which would have helped establish whether the assumed static mechanism was in fact present after a low-temperature deformation.

In summary, the situation for normal metallic alloys is opaque. The measurements are very difficult. At present the bulk of data suggest that the static mechanism is present, at least for large dislocation densities. Useful data would be provided by measurements over a broad range of temperatures and dislocation densities for alloys deformed at both high and low temperatures.

2.4.2. Bismuth

The principle carriers of heat in bismuth at low temperatures are phonons. Thus the problem of subtracting the electronic contribution is largely avoided. A dislocation density of $\simeq 10^{11}$ m^{-2}, introduced by a compressive strain, produced $\kappa_{ph} \simeq 9 \times 10^{3} T^{2.2}$ within the limited measurement range of 1.5 - 4 K [65]. This is close to the T^2 temperature dependence expected for the static phonon-dislocation interaction, but

the magnitude of the measured κ_{ph} is a factor of $\gtrsim 20$ too small. The authors conclude that a dynamic interaction is present, but data to lower temperatures would provide more convincing evidence.

2.5. Related measurements

Several diverse properties may provide additional insight into the interactions between thermal phonons and dislocations.

2.5.1. Scattering from grain boundaries

A grain boundary may be considered to be an ordered array of dislocations. Early measurements on low-angle grain boundaries in NaCl [66] and silicon [67] indicated a strong and possibly dynamic scattering of thermal phonons. However, more recent systematic measurements of κ_{ph} in samples of LiF and NaCl containing measured densities of low-angle grain boundaries failed to detect any phonon-scattering mechanism stronger than that which would be expected for a static interaction [25]. The same results were obtained from measurements involving ballistic phonons in crystals of silicon containing a single grain boundary [68]. It is possible that the dislocations in the grain-boundaries of the NaCl and LiF samples were fully pinned by impurities during the thermal treatment used to form the boundaries. Hence, any dynamic interaction would be repressed, see Sec. 2.1.1. For silicon, attempts were made by heat treatment to disperse any impurities which might pin the dislocations on the grain boundary, but the phonon scattering magnitude did not change. In brief, there is no conclusive evidence that dislocations in grain boundaries scatter thermal phonons by other than the static mechanism.

2.5.2. Scattering from sample surfaces

The scattering of phonons from the surface of a sample is diffusive in both direction and energy if the surface has been slightly abraided. That is, the surface is "black" to phonons in an optical sense [42]. There is considerable evidence that much of the diffusive scattering is caused by defects, such as dislocations located immediately beneath the surface [42], rather than by the topographic roughness of the surface as is generally assumed [69]. Indeed, such diffusive boundary scattering has not been detected at the abraided surface of glassy materials [42], materials which do not support ordinary dislocations. Also, a room temperature γ-irradiation can reduce the diffusive boundary scattering in NaCl [70] and in LiF [29]. These facts suggest that a dynamic phonon-dislocation interaction is active in "boundary" scattering in crystals, the dislocations having been introduced by abrasion.

2.5.3. Specific heat measurements

The presence of a dynamic phonon scattering process requires that the localized vibrational mode of the dislocation contribute to the specific heat. Several measurements have been made on pure metals at large dislocation densities [71]. The change in specific heat caused by cold-rolling a sample is small, $\simeq$ 1%. The results for copper [72] are shown by the solid curve in Fig. 11. The dashed line has been calculated from the vibrating-string model of Granato using the measured dislocation density of $\simeq 2 \times 10^{15}$ m^{-2}. The average length of dislocation segment free to flutter which is obtained from this fit is $L \simeq 3 \times 10^{-8}$ m. This value is close to the estimate of 3.5×10^{-8} m assuming that dislocations

pin dislocations at large dislocation densities, i.e. $L \approx N^{-1/2}$. This value of L is also similar in magnitude to those deduced from other measurements at thermal vibrational amplitudes, such as thermal conductivity measurements on deformed LiF [28].

If the above interpretation is correct, the dislocation resonance can persist at very large dislocation densities. This is contrary to the conclusion derived from most thermal conductivity measurements. It would suggest that the dynamic phonon scattering process itself is in some way weakened by large dislocation densities, which is equivalent to stating that the local vibrational mode associated with the dislocation thermalizes or relaxes less rapidly to the phonon bath. Hence only the static-scattering process would be observed in the thermal conductivity measurements of highly deformed samples.

2.5.4. Amorphous materials

Several authors [73] have suggested that the amorphous state is basically the crystalline state containing a very large density of dislocations, $N \approx 10^{18}\ m^{-2}$. Indeed the thermal conductivities of glassy materials do vary as T^2 below 1 K [74], and it has been suggested that this is due to the static phonon-dislocation interaction [75,76] even though a deviation from a T^2 dependence might be expected as such large dislocation densities (See Sec. 1.2.1). It is also observed that the specific heats of amorphous materials are anomalously large below 1 K [74]. Since the specific heat of deformed copper (Sec. 2.5.3.) indicates that dislocation resonances may persist to large N, the anomalous specific heats of glasses

might be explained by dislocation resonances of the vibrating-string type [76]. Nevertheless, available information [77,78] suggests that the small κ_{ph}, the large specific heat and several other unusual properties of glasses are all caused by the same set of localized excitations which have only two allowed energy levels. Such excitations are not compatible with the classical mechanical oscillator intrinsic to a vibrating-string model.

2.5.5. Ultrasonic measurements

The damping of dislocation motion at high temperatures (80-300 K) and at ultrasonic frequencies and amplitudes can be interpreted in terms of the scattering of thermal phonons by the moving dislocations. The results for NaCl [32,79], LiF [32], and copper [80] are in qualitative agreement with the static scattering model in which, as in earlier Sections of this chapter, the largest interaction between phonon and dislocation is utilized. Only the static interaction is expected to be important in these ultrasonic measurements at high temperatures. This is because the frequency dependence of the phonon-dislocation interaction for thermal phonons in the static interaction varies as ω^1 while that of the dynamic interaction, well above the resonance, varies as ω^{-z}, $z > o$ [81]. Hence, in the dominant-phonon approximation, dynamic scattering of high frequency thermal phonons appropriate to a measuring temperature of $\gtrsim$ 80 K should be negligible.

2.5.6. High-frequency resonances

Infrared measurements have revealed in LiF (and other materials) a local vibrational mode at a frequency of $\approx 10^{13}$ Hz believed to be associated with dislocations since, to detect this mode, the incident electromagnetic

radiation had to be polarized parallel to the dislocation slip plane [82]. These high frequency resonances should provide information on the microscopic topology of dislocations. However, the frequencies are too large to influence the scattering of low temperature phonons.

An unsuccessful attempt was made to detect the possible dislocation resonance in aluminum by measuring the electrical resistivity in the normal metal [83]. A resonance would occur near 1 K in the dominate-phonon approximation (Sec. 2.32). The dynamic electron-dislocation interaction, if present, was too weak to detect. On the other hand, measurements of electrical resistivity in copper and aluminum (and their alloys) have revealed an anomaly near 25 K in deformed samples [84]. This has been interpreted as arising from the scattering of conduction electrons by a vibrational dislocation mode occuring at a frequency of $\approx 2 \times 10^{12}$ Hz. However, it is more likely that the electrons are scattered by localized electronic levels associated with the dislocations [85].

3. Conclusions

There is convincing experimental evidence that the phonon-dislocation interaction in LiF is a dynamic mechanism for fresh, unpinned dislocations. The effect of pinning suggests that the dynamic mechanism involved is a fluttering of dislocation segments as depicted in a vibrating-string model.

The phonon-dislocation scattering mechanism in many superconducting metals containing a small density of dislocations is described in temperature dependence and in magnitude by a dynamic interaction. There is not, however, sufficient experimental information to distinguish between the various suggested dynamic mechanisms, i.e. a string model [22], an internal mode of a dislocation dipole [23,24] or a dissociated dislocation [26,27],

a quantum-mechanical tunneling [86,87], or oscillations in a Peierls-Nabarro lattice potential [28]. As the dislocation density increases, the phonon-dislocation interactions in tantalum and in niobium seem to become more characteristic of the static mechanism.

The phonon-dislocation interaction in covalently bonded germanium and silicon crystals is characteristic of static scattering. By static scattering we mean explicitly the model in which the phonon scatters from the static strain fields of isolated, sessile dislocations. An appropriate example is the calculation by Klemens. The magnitude of the scattering is in remarkably good agreement with this theory if the largest theoretical scattering cross-sections are utilized. However, selection of the largest theoretical cross-section appears to be somewhat arbitrary and is worthy of a clarifying theoretical investigation.

In metallic alloys, most data at large dislocation densities suggest that the static mechanism of phonon scattering is present. Again, there is good agreement with the theoretical static-scattering model provided the largest theoretical cross-sections are adopted. Also, there is a questionable indication that the interaction becomes more dynamic in character as the dislocation density is reduced.

If, in fact, the dynamic interaction is suppressed at large dislocation densities, it is not obvious how this may occur. Measurements of the specific heat of deformed copper indicate that the localized vibrational modes of the dislocations may persist at large dislocation densities. A reduction in the dynamic phonon-dislocation scattering cross-section at large dislocation densities would then be required to

explain why only the static interaction is observed in the thermal conductivity. Alternatively, measurements of thermal conductivity in deformed tantalum suggest that the resonant frequency of the dislocation mode is increased with increased dislocation density. Thus, for large dislocation densities, the resonance may be pushed to very high frequencies leaving only the static mechanism to scatter the low frequency phonons which are dominant at temperatures below $\approx$ 2 K.

It has been stated in the literature that the thermal conductivity technique is a highly desirable, nondestructive method for studying defect structures in solids. Unfortunately, and contrary to the claims of some authors, the present understanding of the phonon-dislocation interaction is too primitive to allow the thermal conductivity of deformed bodies to be used as a definitive, diagonistic tool. Additional experimental and theoretical efforts need to be directed to a delination of the basic phonon-dislocation interactions.

Acknowledgements

The author's work on the phonon-dislocation interaction has been supported by the U. S. Department of Energy under Contract DE-AC02-76ER01198 A portion of this paper was prepared while the author was a visitor at the Aspen Center for Physics.

Figure Captions

Fig. 1. Schematic arrangement of a sample mounted for thermal conductivity measurements. The symbols are discussed in the text.

Fig. 2. Thermal conductivity, κ_{ph}, of deformed LiF crystals, divided by the thermal conductivity κ_B of the undeformed sample. The dashed line at 1.0 indicates no change relative to the undeformed state. A, deformed by shearing as indicated by the inset to the figure, no γ-irradiation; B, sample A following deformation and 1000 R of γ-irradiation; C, 136,000 R (from Ref. 28). D, deformed by bending about [001], no γ-irradiation; E, sample D following deformation and 180,000 R of γ-irradiation (from Ref. 29). Such irradiation does not change the κ_{ph} of an undeformed sample.

Fig. 3. Bolometer output versus time for ballistic phonons excited by a heat pulse in LiF. The arrival times of the longitudinal (L), fast-transverse (FT) and slow-transverse (ST) acoustic phonons are indicated by the arrows. A, undeformed sample; B, sample deformed by shearing as in the inset of Fig. 2. The dotted lines indicate the magnitude of the background signal caused by the diffusive scattering of longitudinal and fast transverse phonons. From Ref. 28.

Fig. 4. Phonon thermal conductivity, κ_{ph}, of deformed LiF, divided by the thermal conductivity κ_B of the undeformed sample. Note that the vertical scale is logarithmic, whereas that in Fig. 2 is linear. The solid and dotted curves represent two different samples with different dislocation densities. A, C, deformed by compression; B, D, the samples A, C, after thermal treatment at 300°C (from

Ref. 36). The curves rise at $T \gtrsim 10$ K since other phonon-scattering processes that occur above the peak in κ_{ph} begin to mask the scattering caused by dislocations, see Ref. 29.

Fig. 5. Phonon mean free path ℓ in germanium related to an increase in dislocation density of $\approx 2 \times 10^{13}$ m^{-2}. Solid curve, from Ref. 43; dotted line, lower limit on ℓ deduced from Ref. 44; dashed curve, calculated from the static-interaction model. The more rapid decrease in the solid curve near 10 K is caused by other phonon scattering processes which begin to appear near the peak in κ_{ph}.

Fig. 6. Phonon mean free path ℓ in superconducting tantalum. The phonon scattering at temperatures below 1 K is caused by dislocations, that above $\approx$ 1 K is due to conduction electrons. A, B, C, from Ref. 39, deformed by bending; D from Ref. 48, cold-rolled; E (solid curve), from Ref. 49, not intentionally deformed but containing a dislocation density of $\approx 10^{11}$ m^{-2}.

Fig. 7. Phonon mean free path ℓ in superconducting aluminum. Curve A, two different measurements on a rod deformed at room temperature. Curve B, foil deformed at low temperature. From Ref. 50.

Fig. 8. Phonon mean free path ℓ in superconducting lead. A, deformed at room temperature, Ref. 39. B, deformed at low temperature, Ref. 51. C, deformed at 4 K, Ref. 52. The dashed line is the prediction of the Granato vibrating-string model for a dislocation density appropriate to curve A. The abrupt decrease in ℓ above 2 K is caused by conduction electrons.

Fig. 9. Phonon mean free path ℓ in superconducting niobium. A, B, two rods deformed by bending at room temperature (from Ref. 3). C, rod deformed at 195 K; rods deformed at 300 K and 470 K gave similar results (from Ref. 53). The abrupt decrease in ℓ above 2 K is caused by phonon scattering by conduction electrons.

Fig. 10. Phonon mean free path ℓ in copper alloys, multiplied by the measured dislocation density N to simplify comparison. A, composite of several measurements on highly deformed samples; B, composite of several measurements from Ref. 6 on slightly bent samples (small N, hence scattering caused by electrons has been subtracted); C, from Ref. 62.

Fig. 11. The increase in specific heat, ΔC, of copper caused by cold rolling. Solid line represents the experimental results from Ref. 72. The dashed line is a fit to the data using the Granato vibrating-string model.

References

[1]. R. Berman, Thermal Conduction in Solids (Clarendon, Oxford, 1976) and papers cited.

[2]. V. Narayanamurti and R. O. Pohl, Rev. Mod. Phys. 42 (1970) 201.

[3]. A. C. Anderson and S. C. Smith, J. Phys. Chem. Solids 34 (1973) 111.

[4]. M. K. McCurdy, Phys. Rev. B9 (1974) 466.

[5]. Y. Kogure and Y. Hiki, J. Phys. Soc. Jap. 38 (1975) 471.

[6]. J. L. Vorhaus and A. C. Anderson, Phys. Rev. B14, (1976) 3256.

[7]. M. P. Zaitlin and A. C. Anderson, J. Low Temp. Phys. 9 (1972) 467.

[8]. A. C. Anderson and M. E. Malinowski, Phys. Stat. Sol. 37 (1970) K141.

[9]. W. L. Johnson and A. C. Anderson, Rev. Sci. Instrum. 42 (1971) 1296.

[10]. E. P. Roth, J. R. Matey, A. C. Anderson, and D. A. Johns, Rev. Sci. Instrum. 49 (1978) 813.

[11]. J. F. Schooley, J. Phys. (Paris) 39 (1978) C6-1169.

[12]. R. J. Soulen, J. Phys. (Paris) 39 (1978) C6-1166.

[13]. M. Durieux, D. N. Astrov, W.R.G. Kemp, and C. A. Swenson, Metrologia 15 (1979) 57.

[14]. P. G. Klemens, in Solid State Physics, Vol. 7, ed. D. Turnbull and F. Seitz (Academic, New York, 1958), p. 1.

[15]. M. W. Ackerman and P. G. Klemens, J. Appl. Phys. 42 (1971) 968.

[16]. M. W. Ackerman and P. G. Klemens, Phys. Rev. B3 (1971) 2375.

[17]. P. Gruner and H. Bross, Phys. Rev. 172 (1968) 583.

[18]. H. Bross, Z. Physik 189 (1966) 34.

[19]. P. G. Klemens, Can. J. Phys. 35 (1957) 441.

[20]. K. Ohashi and Y. H. Ohashi, Phil. Mag. A38 (1978) 187.

[21]. T. Ninomiya, Equations of Motion of a Dislocation and Interactions with Phonons in: Treatise on Materials Science and Technology, Vol. 8 ed. by H. Herman (Academic, New York, 1975) p. 1, the papers cited therein.

[22]. A. Granato, Phys. Rev. 111 (1958) 740; J. A. Garber and A. V. Granato, J. Phys. Chem. Solids 31 (1970) 1863.

[23]. T. Matsuo and H. Suzuki, J. Phys. Soc. Jap. 43 (1977) 1974.

[24]. G. A. Kneezel, Ph.D. Thesis, University of Illinois, 1980 (unpublished).

[25]. E. P. Roth and A. C. Anderson, Phys. Rev. B17 (1978) 3356.

[26]. H. Kronmuller, Phys. Stat. Sol. B52 (1972) 231.

[27]. F. Kroupa, Phys. Stat. Sol. B84 (1977) 725.

[28]. A. C. Anderson and M. E. Malinowski, Phys. Rev. B5 (1972) 3199.

[29]. E. P. Roth and A. C. Anderson, Phys. Rev. B20 (1979) 768.

[30]. R. Berman and J.C.F. Brock, Proc. Roy. Soc. 289A (1965) 46.

[31]. Ya. M. Soifer, Phys. Stat. Sol. A4 (1971) 333.

[32]. F. Fanti, J. Holder, and A. V. Granato, J. Acoust. Soc. Amer. 45 (1969) 1356.

[33]. L. Kemter and H. Strunk, Phys. Stat. Sol. A40 (1977) 385.

[34]. M. Peach and J. Koehler, Phys. Rev. 80 (1950) 436.

[35]. A. Taylor, H. R. Albers, and R. O. Pohl, J. Appl. Phys. 36 (1965) 2270.

[36]. T. Suzuki and H. Suzuki, J. Phys. Soc. Jap. 32 (1972) 164.

[37]. K. Ohashi, J. Phys. Soc. Japan 24 (1968) 437.

[38]. D. Eckhardt and W. Wasserbach, Phil. Mag. A37 (1978) 621.

[39]. S. G. O'Hara and A. C. Anderson, Phys. Rev. B10 (1974) 574.

[40]. P. W. Levy, P. L. Mattern, K. Lengweiler, and M. Goldberg, Solid State Commun. 9 (1971) 1907.

[41]. S. Ishioka and H. Suzuki, J. Phys. Soc. Jap. (Suppl. II) 18 (1963) 93.

[42]. M. P. Zaitlin, L. M. Scherr, and A. C. Anderson, Phys. Rev. B12 (1975) 4487, and papers cited.

[43]. M. Sato and K. Sumino, J. Phys. Soc. Jap. 36 (1974) 1075.

[44]. M. P. Zaitlin and A. C. Anderson, Phys. Rev. B10 (1974) 580.

[45]. P. G. Klemens, Proc. Phys. Soc. A68 (1955) 1113.

[46]. P. G. Klemens, (private communication).

[47]. M. W. Ackerman, Phys. Rev. B5 (1972) 2751.

[48]. M. Ikebe, N. Kobayoshi, and Y. Muto, J. Phys. Soc. Jap. 37 (1974) 278.

[49]. W. Wasserbach, Phys. Stat. Sol. B84 (1977) 205.

[50]. S. G. O'Hara and A. C. Anderson, Phys. Rev. B9 (1974) 3730.

[51]. P. M. Rowell, Proc. Roy. Soc. A254 (1960) 542.

[52]. L. P. Mezhov-Deglin, J. Phys. (Paris) 39 (1978) C6-1019; Zh. Eksp. Teor. Fiz. 77 (1979) 733.

[53]. W. Wasserbach, Phil. Mag. A38 (1978) 401.

[54]. A. H. Cottrell, Dislocations and Plastic Flow in Crystals, (University, Oxford, 1963) p. 29.

[55]. J. J. Gilman, in Fundamental Aspects of Dislocation Theory, ed. J. A. Simmons, R. de Wit and R. Bullough, Nat. Bur. Stds. Spec. Publ, #317 (1970) p. 459.

[56]. W.R.G. Kemp, P. G. Klemens, and R. J. Tanish, Phil. Mag. 4 (1959) 845.

[57]. J. N. Lomer and H. M. Rosenberg, Phil. Mag. 4 (1959) 467.

[58]. P. Charsley, J.A.M. Salter, and A.D.W. Leaver, Phys. Stat. Sol. 25 (1968) 531.

[59]. Y. Kogure and Y. Hiki, J. Phys. Soc. Jap. 39 (1975) 698.

[60]. R. Zeyfang, Phys. Stat. Sol. 24 (1967) 221.

[61]. R. W. Klaffky, N. S. Mohan, and D. H. Damon, Phys. Rev. B11 (1975) 1297.

[62]. M. Kusunoki and H. Suzuki, J. Phys. Soc. Jap. 26 (1969) 932.

[63]. T. K. Chu, J. Appl. Phys. 46 (1975) 5101.

[64]. P. Charsley and M.H.S. Rahim, Phys. Stat. Sol. A34 (1976) 533, and papers cited.

[65]. T. Matsuo and H. Suzuki, J. Phys. Soc. Jap. 41 (1976) 1692.

[66]. K. A. McCarthy, in Proc. of the Ninth International Conf. on Low Temp. Physics, eds. J. G. Daunt, D. O. Edwards, F. J. Milford, and M. Yaqub (Plenum, New York, 1965) p. 1155.

[67]. K. Hubner and W. Shockley, in Proc. International Conf. Phys. Semicond., ed. A. C. Stickland (Inst. Phys. and Phys. Soc., London, 1962) p. 157.

[68]. E. P. Roth and A. C. Anderson, Phys. Stat. Sol. B93 (1979) 261.

[69]. Th. F. Nonnenmacher and R. Wunderle, Phys. Stat. Sol. B91 (1979) 147, and papers cited.

[70]. C.-K. Chau and M. V. Klein, Phys. Rev. B1 (1970) 2642.

[71]. V. M. Pulovov, N. A. Tulina, and N. M. Gavrilov, Sov. J. Low Temp. Phys. 3 (1977) 604, and papers cited.

[72]. J. Bevk, Phil. Mag. 28 (1973) 1379.

[73]. H. Koizumi and T. Ninomiya, J. Phys. Soc. Jap. 44 (1978) 898, and papers cited.

[74]. R. C. Zeller and R. O. Pohl, Phys. Rev. B4 (1971) 2029.

[75]. T. Scott and M. Giles, Phys. Rev. Lett. 29 (1972) 642.

[76]. P. R. Couchman, C. L. Reynolds, and R.M.J. Cotterill, Nature 264 (1976) 534.

[77]. T. L. Smith, P. J. Anthony and A. C. Anderson, Phys. Rev. B17 (1978) 4997.

[78]. D. S. Matsumoto, C. L. Reynolds, and A. C. Anderson, Phys. Rev. B19 (1979) 4277.

[79]. A. Hikata, J. Deputat, and C. Elbaum, Phys. Rev. B6 (1972) 4008.

[80]. K. M. Jassby and T. Vreeland, Phys. Rev. B8 (1973) 3537.

[81]. V. I. Alshits and Yu. M. Sandler, Phys. Stat. Sol. B64 (1974) K45.

[82]. B. M. Tashpulatov, V. I. Vettegren, and I. I. Novak, Sov. Phys. Solid State 20 (1978) 111.

[83]. S. G. O'Hara and A. C. Anderson, Phys. Stat. Sol. B67 (1975) 401.

[84]. G. I. Kulesko, Sov. Phys. JETP 48 (1978) 85, and papers cited.

[85]. T. Endo and T. Kino, J. Phys. Soc. Jap. 46 (1515) 1979.

[86]. J. M. Galligan and T. Oku, Acta. Met. 19 (1971) 223.

[87]. V. D. Natsik, Sov. J. Low Temp. Phys 5 (1979) 191.

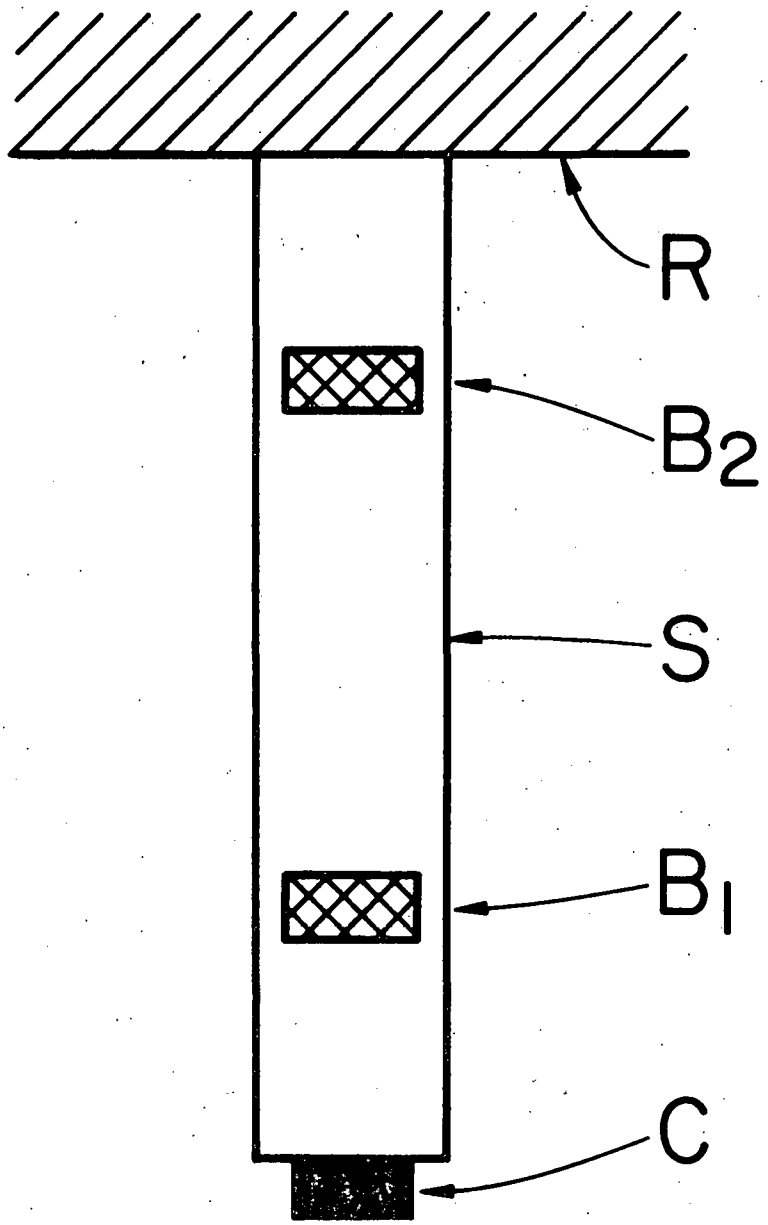

Fig. 1.

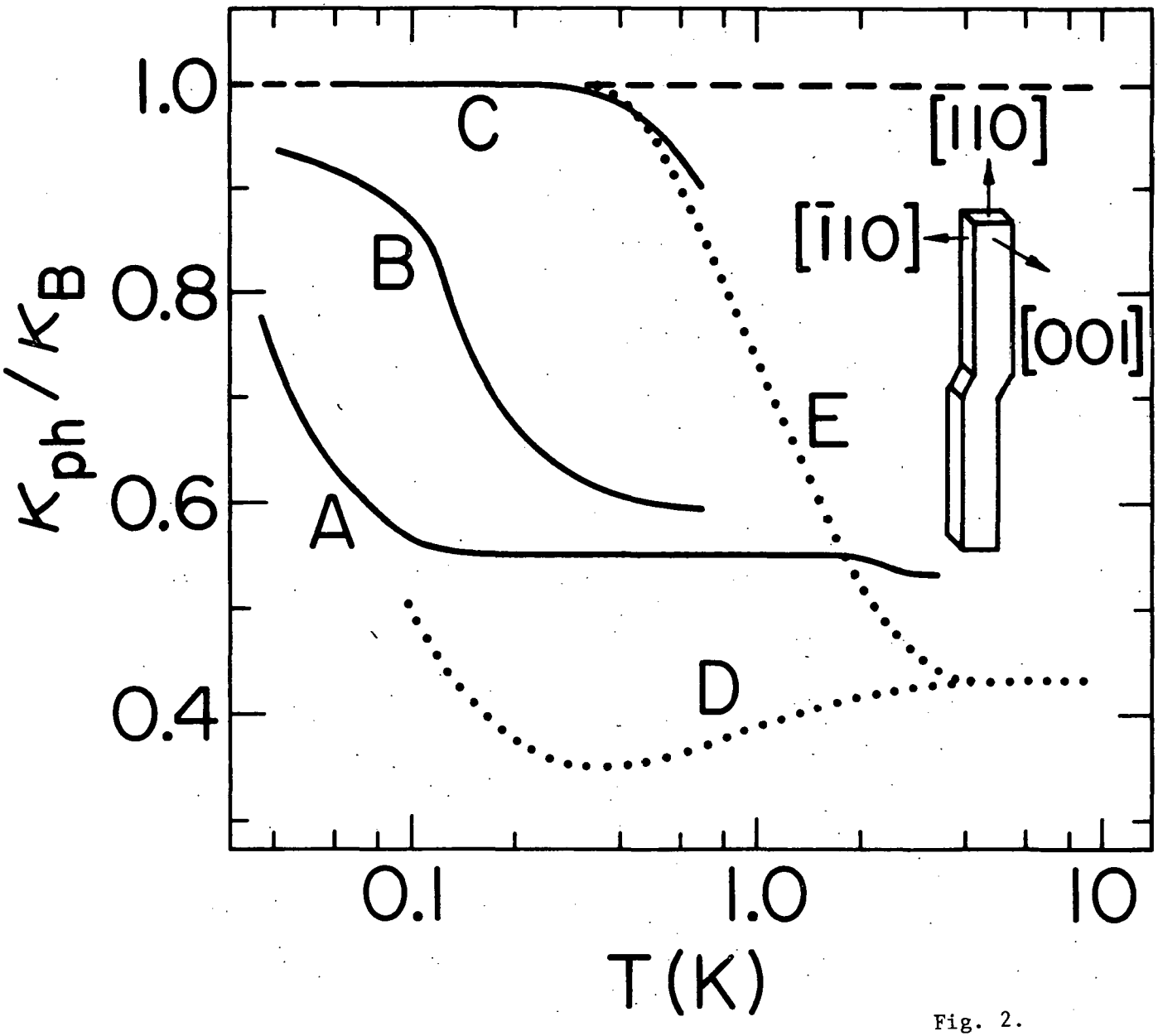

Fig. 2.

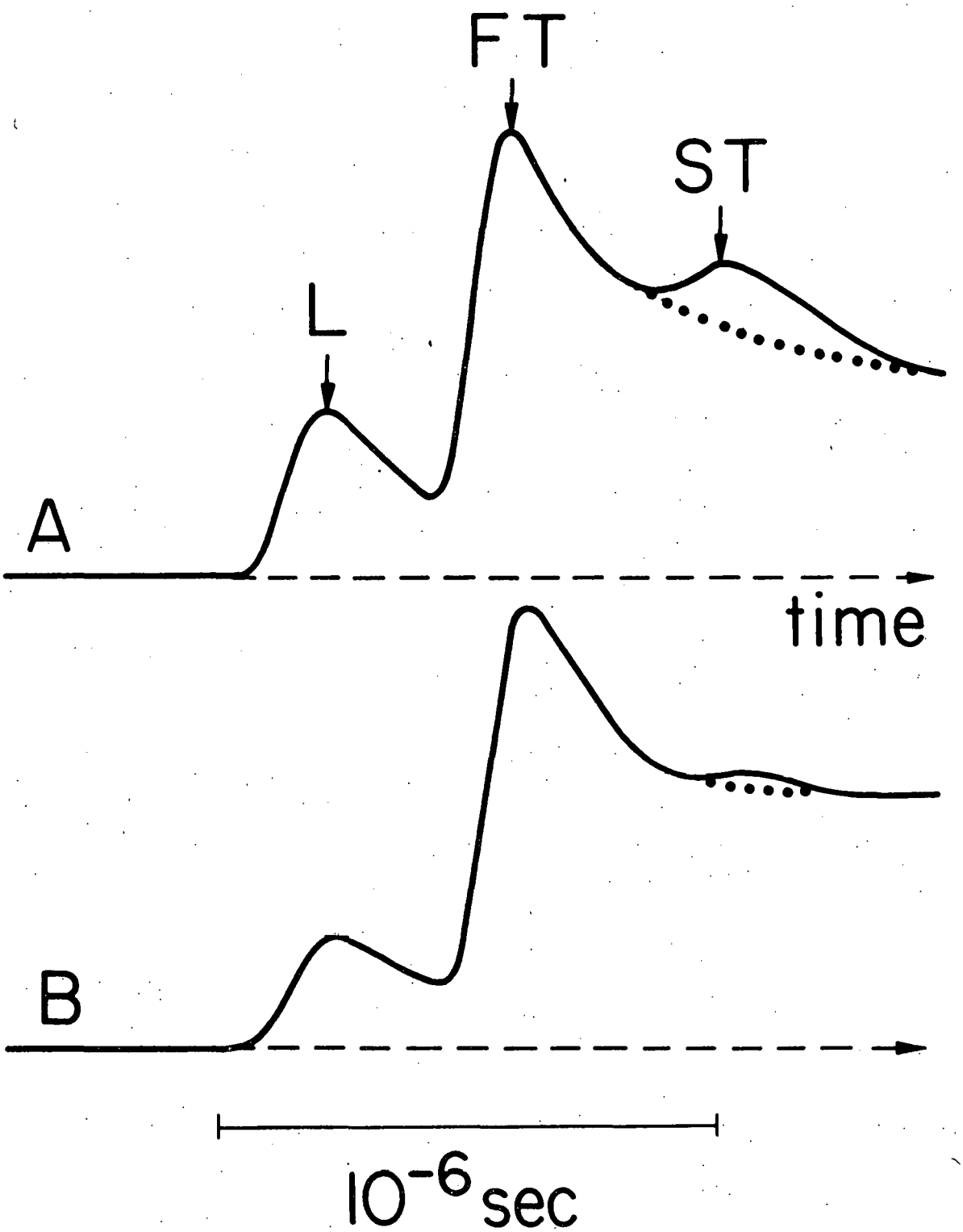

Fig. 3.

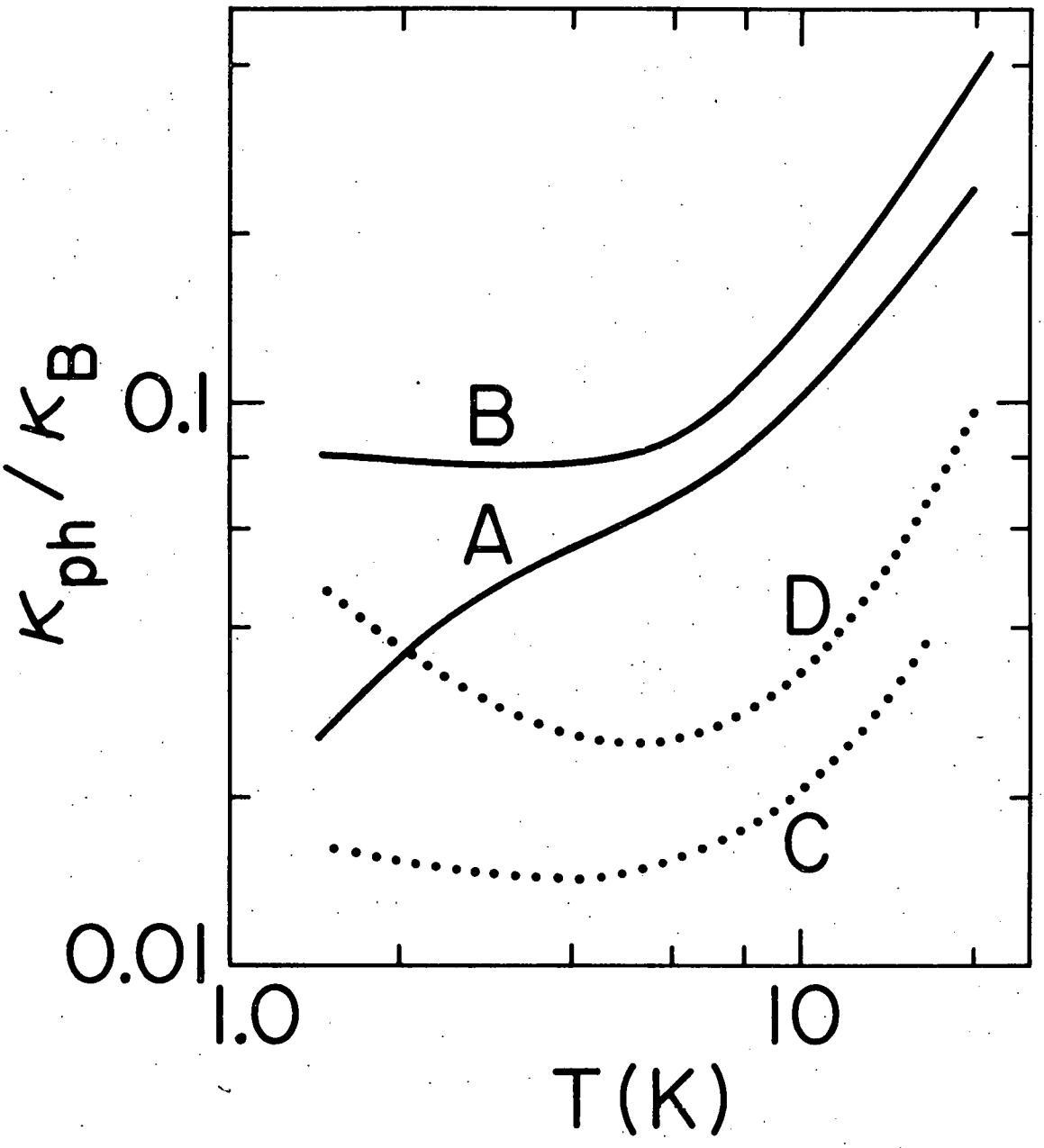

Fig. 4.

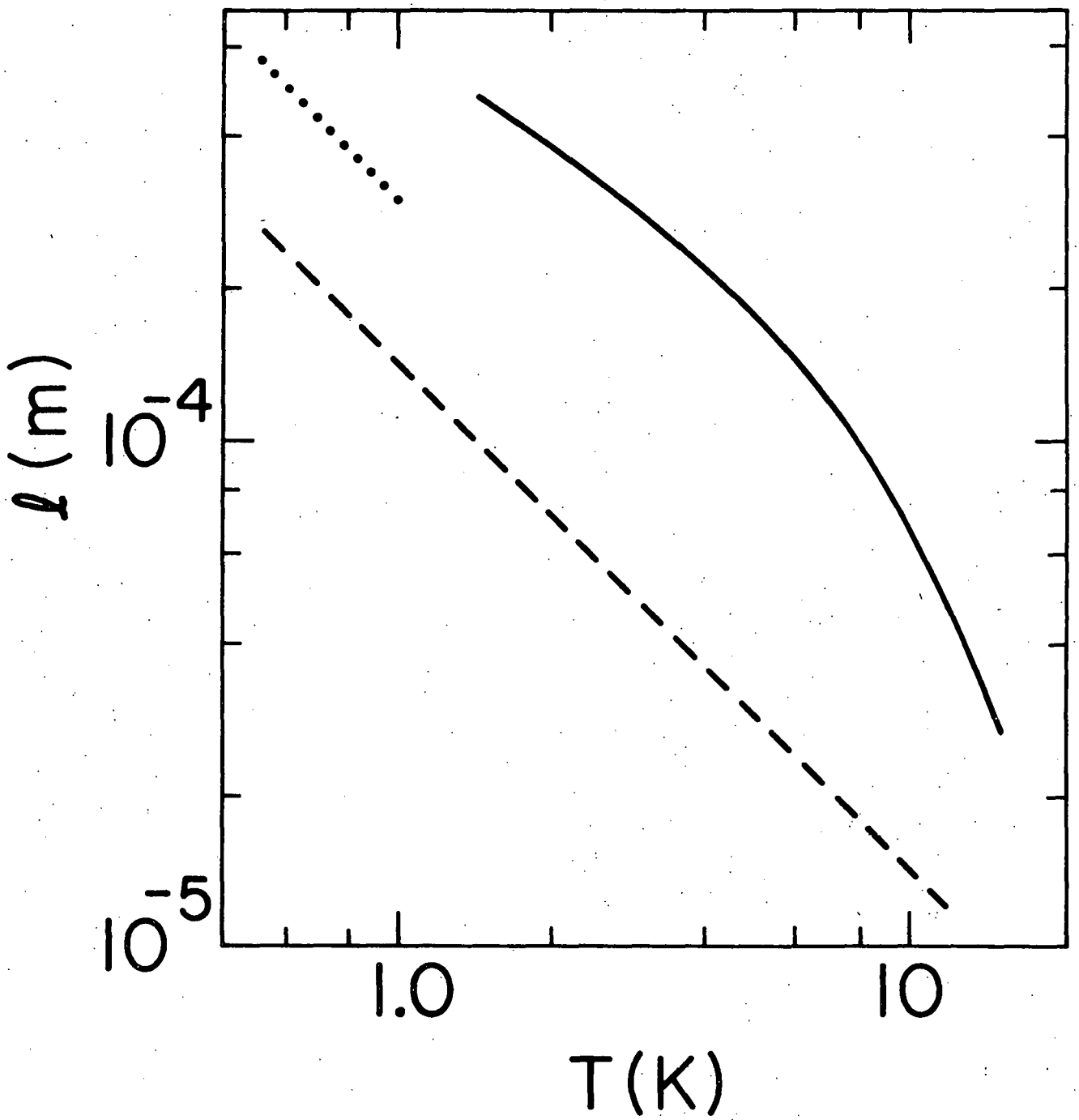

Fig. 5.

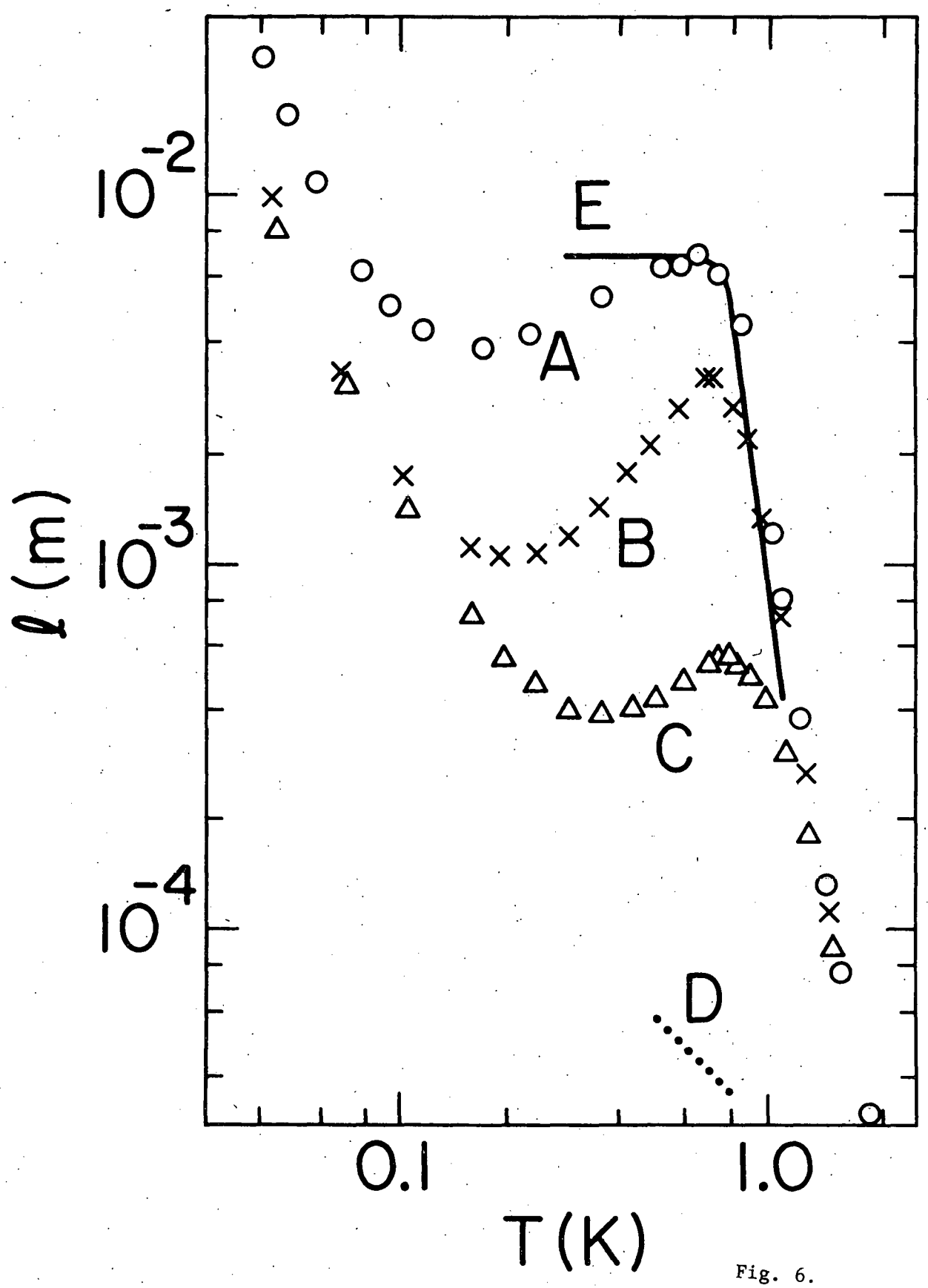

Fig. 6.

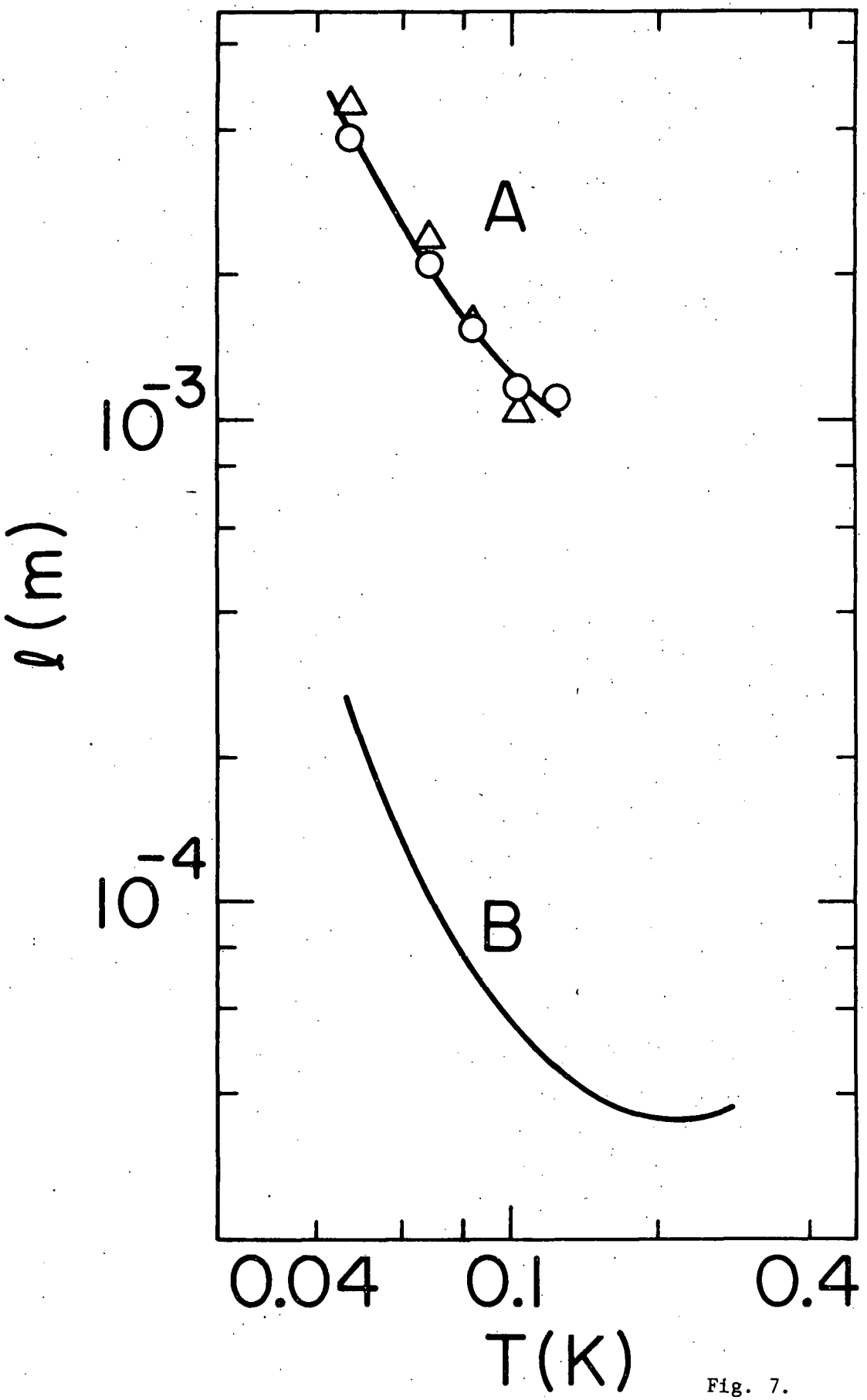

Fig. 7.

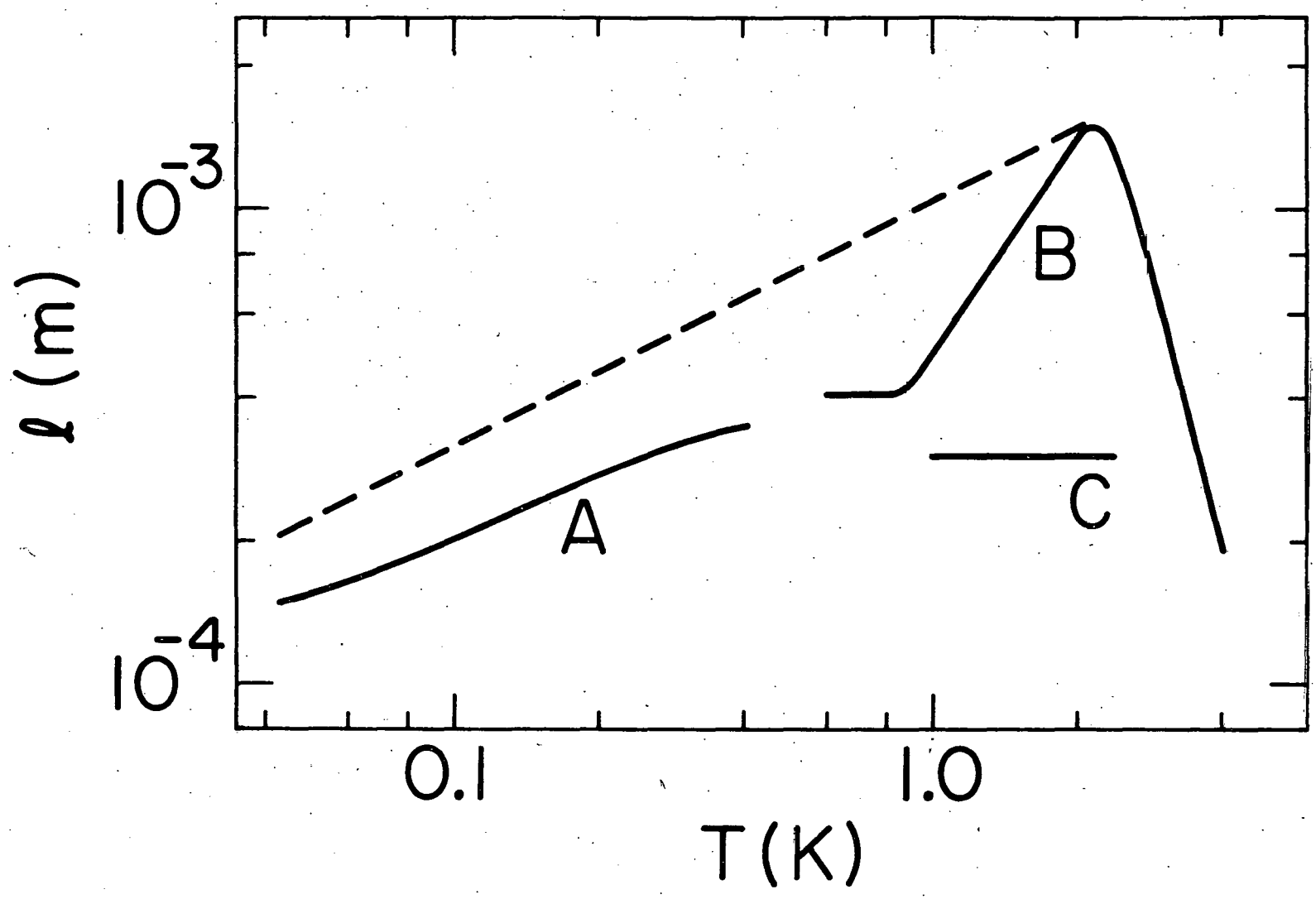

Fig. 8.

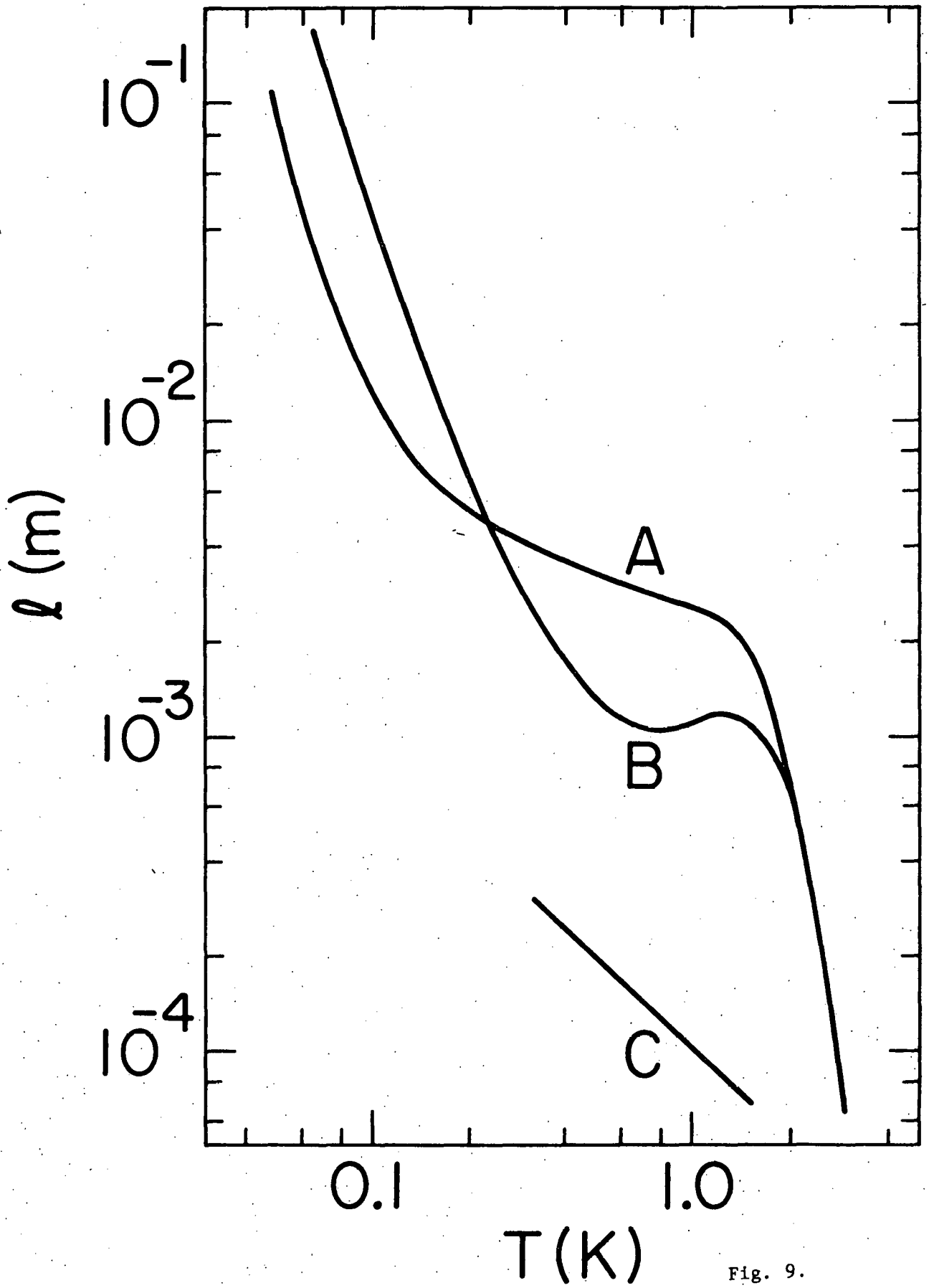

Fig. 9.

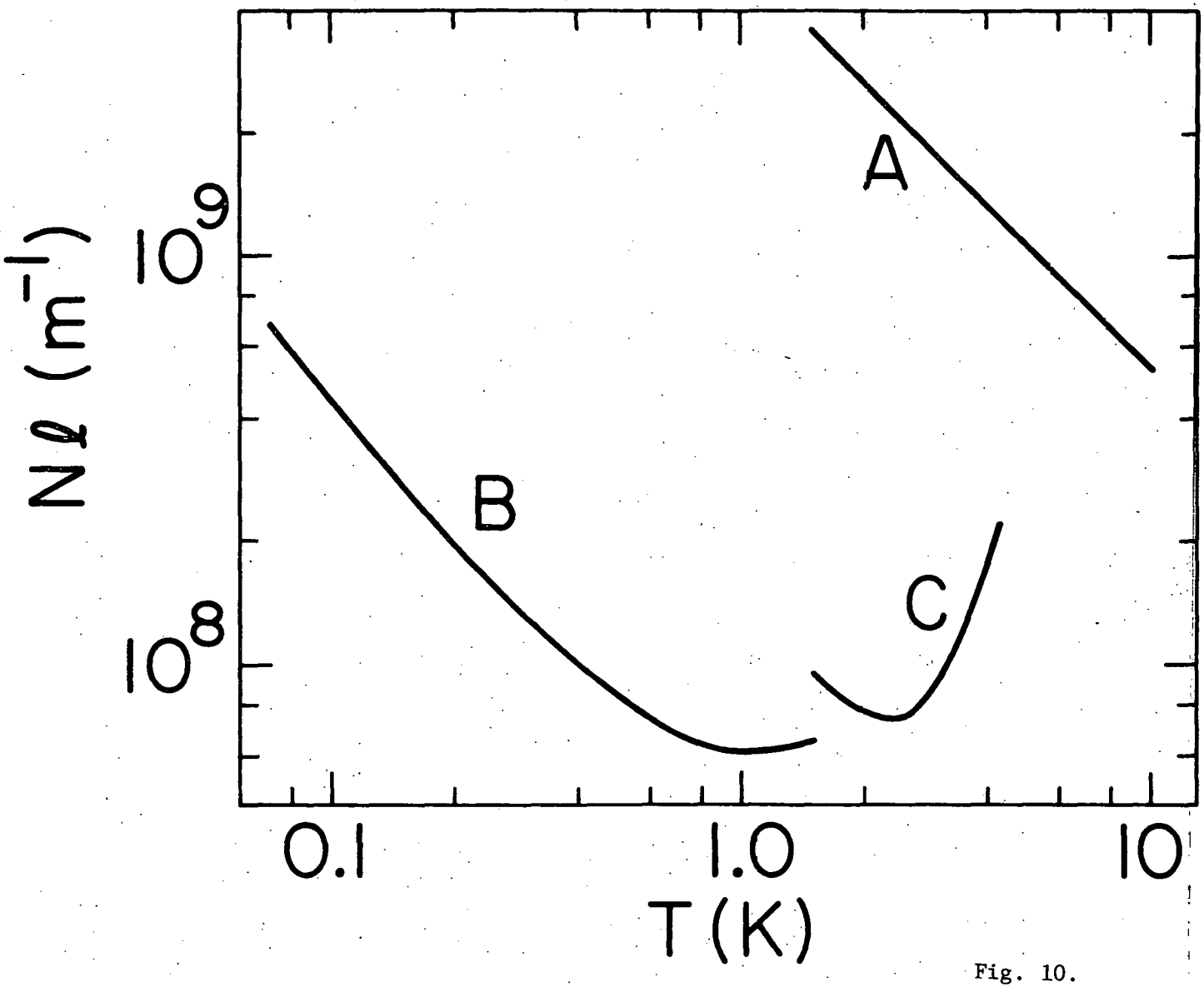

Fig. 10.

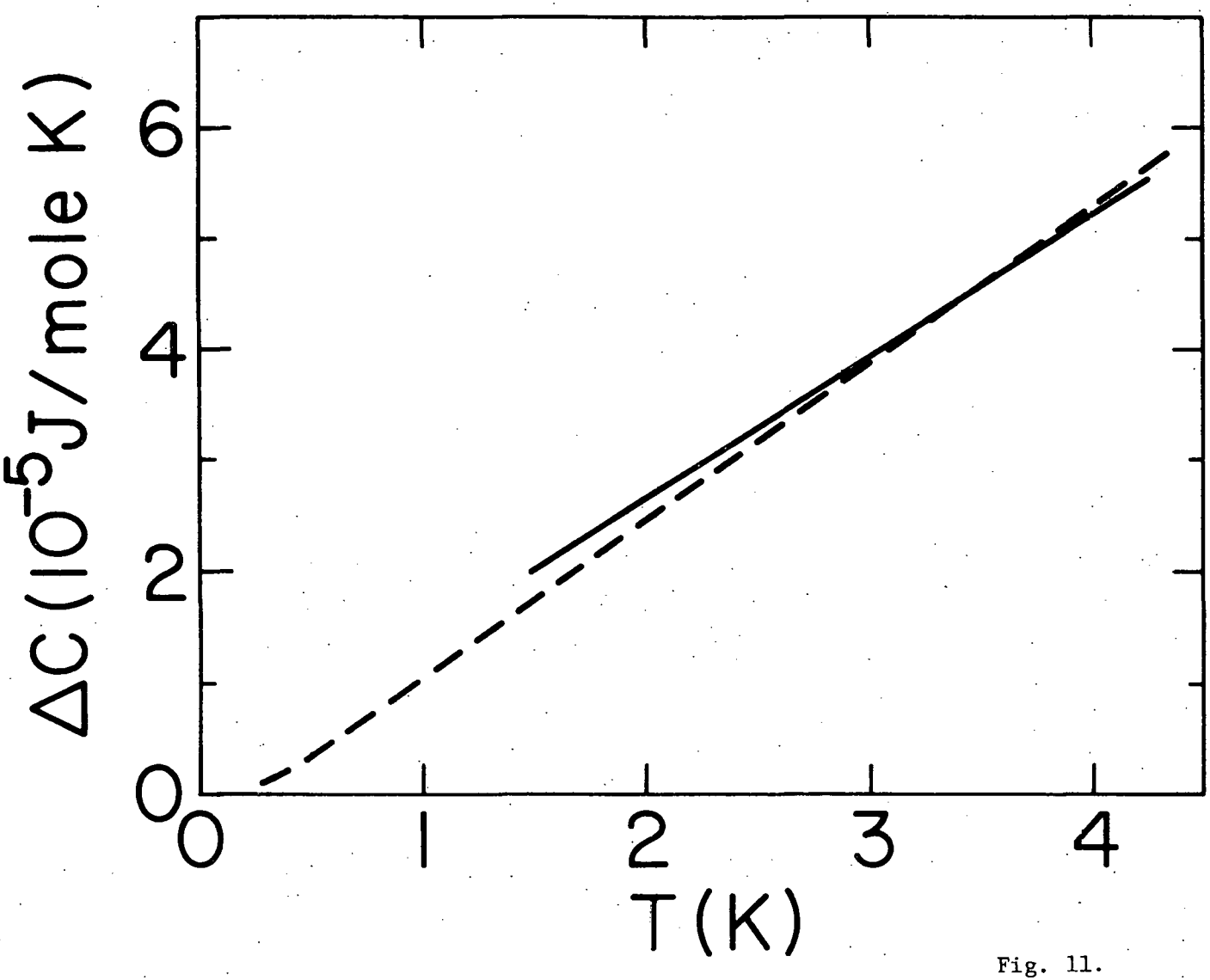

Fig. 11.